QED calculation of transition probabilities in two-electron ions

Oleg Yu. Andreev,[1,2] Leonti N. Labzowsky,[1,3] and Günter Plunien[2]
[1]*V. A. Fock Institute of Physics, Faculty of Physics, St. Petersburg State University, Ulyanovskaya 1, Petrodvorets, St. Petersburg 198504, Russia*
[2]*Institut für Theoretische Physik, Technische Universität Dresden, Mommsenstraße 13, D-01062 Dresden, Germany*
[3]*Petersburg Nuclear Physics Institute, Gatchina, St. Petersburg 188300, Russia*
(Received 20 March 2008; revised manuscript received 23 September 2008; published 23 March 2009)

An accurate QED calculation of transition probabilities for the low-lying two-electron configurations of multicharged ions is presented. The calculation is performed for the nondegenerate states $(1s2s)\ ^3S_1$, $(1s2p_{3/2})\ ^3P_2$ ($M1$ and $M2$ transitions, respectively) and for the quasidegenerate states $(1s2p)\ ^1P_1$, $(1s2p)\ ^3P_1$ ($E1$ transitions) decaying to the ground state $(1s1s)\ ^1S_0$. Two-electron ions with nuclear-charge numbers $Z=10-92$ are considered. The line profile approach is employed for the description of the process in multicharged ions within the framework of QED.

DOI: 10.1103/PhysRevA.79.032515 PACS number(s): 31.10.+z

I. INTRODUCTION

Highly charged ions (HCIs), in particular, two-electron HCIs considered in the present work are under intensive experimental and theoretical investigation during the last decades. In HCI the electrons are propagating in the field of the nucleus, which exceeds in strength all other external electric fields accessible in laboratories. This allows for tests of QED in strong electric fields. The most precise experimental data have reached relative levels of accuracy of about 1% in one-electron ions (the measurement of the binding-energy shift, i.e., the difference between the electron binding energy and the Dirac point-nucleus value for this energy, ground state, $Z=92$ [1], about 0.4% in two-electron ions (the measurement of binding energy of one electron in the two-electron ion, ground state, $Z=92$ [2]), and about 0.03% in three-electron ions (the measurements of the $2p_{1/2}-2s_{1/2}$ energy difference for the first excited and ground states, $Z=92$) [3]. In the theoretical studies of the few-electron HCI such a level of accuracy requires the inclusion of the second-order (two-loop) radiative corrections as well as the screening of the first-order (one-loop) radiative corrections. The nuclear size, nuclear recoil, and even the nuclear polarization corrections appear to be of importance as well. What concerns the interelectron interaction corrections, the first-, second-, and partly third-order corrections should be accounted for in high-Z HCI. For intermediate Z values and especially for the quasidegenerate energy levels (see below), the inclusion of the interelectron interaction corrections to all orders, at least within a simplified treatment, becomes necessary. The existing experimental data for the transition probabilities are less accurate (3% for $Z=54$ [4]) but also require from theory to take into account the interelectron interaction and the lowest-order radiative corrections. Moreover, HCI can be used for the investigation of fundamental problems beyond QED: first, for testing the standard model via the observation of parity nonconservation (PNC) effects in HCI. Various suggestions on this subject were made in [5] for one-electron HCI, in [6–11] for two-electron HCI, and in [12,13] for four- and five-electron HCIs, respectively. Regarding two-electron HCI such proposals are based exclusively on the crossings of the energy levels with opposite parity at some Z values. For example, according to the recent calculation [14] the energy-level splitting $\Delta E=E(2\ ^3P_0)-E(2\ ^1S_0)$ for He-like Gd ($Z=64$) amounts to $\Delta E=0.04\pm0.74$ eV. Since the PNC effect is proportional to $\eta=\mathrm{Re}\{\Delta E-i\Gamma/2\}^{-1}=\Delta E/(\Delta E^2+\Gamma^2/4)$, where $\Gamma=0.016$ eV is the $2\ ^3P_0$ level width, the relative PNC effect can be unprecedently large ($\eta=0.05$ for $\Delta E=\Gamma/2$) or exactly zero for ($\Delta E=0$). To eliminate the uncertainty in calculations of the energy splitting ΔE the full account for the two-loop radiative corrections and the more accurate treatment of the interelectron interaction become indispensable. The evaluation of the PNC effects also demands a most precise knowledge of the transition probabilities (level width). Second, it was proposed to use HCI for the search of the variation in fundamental constants [15,16]. Again the precise knowledge of the level crossings and transition probabilities is needed for this purpose [15,16]. In many cases the two-electron ions are preferable for performing the corresponding experiments (see, e.g., [9,15]). Therefore, it is necessary to develop adequate and accurate methods, which allow for predictions of energy levels, transition probabilities, and other characteristics of two-electron HCI with utmost precision.

The most investigated properties of HCI are the energy levels of the electron configurations. Since more than 40 years in the numerous theoretical works a large variety of different methods based on the relativistic many-body theory (RMBT) and QED was suggested and employed in practical calculations. A short survey of these methods in a historical retrospective was presented recently in [17]. A common property of all these methods is that they are exact to all orders in the parameter αZ (α is the fine-structure constant and Z is the nuclear-charge number). In many-electron systems the expansion in αZ implies an expansion with respect to the relativistic parameter $\bar{v}/c$ ($\bar{v}$ is the mean velocity of an atomic electron and c is the speed of light), so that the αZ-expansion methods can be only applied to nonrelativistic systems (low-Z atoms and ions). The relativistic Dirac-Hartree-Fock (RDHF) method [18] and its natural extensions such as multiconfigurational RDHF (MC-RDHF) [19] or a coupled-cluster method based on the RDHF (CC-RDHF) ap-

proximation [20] were widely used in calculations performed for particular ion species. Within these methods the one-electron part of the many-body Hamiltonian is treated exactly as well as the Coulomb part of the interelectron interaction Hamiltonian. Only the Breit part of the interaction Hamiltonian is treated approximately. The validity of this approach was analyzed thoroughly in [21–23]. For few-electron ions with high-Z values the application of the perturbation theory (PT) with respect to the interelectron interaction becomes possible since the interelectron interaction is of the order of $1/Z$ compared to the binding energy [24]. This feature of the many-electron atomic systems is exploited in the most powerful non-QED methods for the evaluation of the properties of HCI in the relativistic many-body perturbation-theory (RMBPT) approach [25]. By means of this method the most extensive calculations of the energy levels in two-electron HCI within a wide range of nuclear-charge numbers Z were performed [26]. Still, compared to the exact QED theory this method suffers from the lack of the negative-energy contributions (though these contributions can be introduced with the special nontrivial efforts [27–29]) from the approximate treatment of the Breit interaction (without retardation) and from the neglect of the cross-photon interactions (which represent a special QED effect) in higher orders of perturbation theory. Moreover, the inclusion of radiative QED corrections within the RMBPT approach is possible only with the use of the αZ-expansion expressions [30] which, strictly speaking, are not valid for HCI. During the last few decades several rigorous QED approaches for the evaluation of the various properties of the HCI were formulated. Unlike the non-QED treatments, the application of QED allows for the consequent improvement of the accuracy of calculations. The first QED methods, based on the adiabatic S-matrix approach and the energy shift formula by Gell-Mann and Low [31] (this formula was later adjusted by Sucher [32] to the QED applications), were introduced in [33] and later applied to the various QED calculations by many authors. However, in higher orders of perturbation theory the adiabatic S-matrix approach becomes rather cumbersome due to the necessity of explicit evaluation of the adiabatic limit (when adiabatic parameter tends to zero). More advantageous for these purposes appeared to be the two-time Green's-function (TTGF) method first formulated in [34,35] (see also the recent review [36]). With this approach a large number of calculations concerning the higher-order (two-loop) radiative corrections to the energy levels [37] as well as the first-order radiative corrections to the hyperfine splittings in HCI [38] and to the bound-electron g factors in HCI [39] were performed. An original approach with the covariant generalization of the evolution operator was recently developed in [40,41]. A special QED approach for the evaluation of the different characteristics of the HCI originates from the QED theory of the spectral line profile first developed by Low [42]. The application of the line profile approach (LPA) to the evaluation of the energy level shifts was first formulated in [43]; simple examples were presented in [44]. The LPA possesses all the advantages of the other methods and allows for the evaluation of any higher-order corrections. A most general formulation of the LPA was given in [45–47] with application to the energy-level calculations in HCI (see also the review [17]). In the present paper we apply the LPA to the high-precision calculations of the transition probabilities in HCI.

Because of inherent difficulties, the transition probabilities are less investigated than the energies. This can be explained by the presence of an extra photon line (emitted photon) in the corresponding Feynman graphs and by the poorer convergence of the QED perturbation theory. A calculation of the transition probabilities with respect to the relativistic corrections has been performed by Drake [48,49] within the unified method. The work [48] presents the first relativistic calculation of transition probabilities for the $(1s2s)\ ^3S_1 \rightarrow (1s1s)\ ^1S_0$ transition. The work [49] presents the calculation of transition probabilities for the $(1s2p)\ ^3P_1, ^1P_1 \rightarrow (1s1s)\ ^1S_0$ transitions. A comprehensive review on the transition probabilities for two-electron ions has been presented by Johnson *et al.* [50] about one decade ago, where the transition probabilities for low-lying two-electron configurations have been calculated for ions within the entire range of nuclear-charge numbers Z. In [50] the RMBPT approach was employed. The contribution of the negative-energy states was discussed in [27–29]. The first complete QED evaluation of transition probabilities in HCI with the account for the interelectron interaction and radiative corrections has been presented in [51,52]. The calculation was performed for nondegenerate states for transitions with emission of electric [51] and magnetic [52] photons, respectively.

In this work we present a calculation of the transition probabilities for two-electron ions with nuclear charge $Z=10-100$. The calculation is performed rigorously within the framework of QED. We also present a special technique developed to master the slow convergence of the QED perturbation theory in the case of the ions with intermediate Z values. The calculation is performed for the nondegenerate states $(1s2s)\ ^3S_1$, $(1s2p_{3/2})\ ^3P_2$ ($M1$ and $M2$ transitions, respectively) and for the quasidegenerate levels $(1s2p)\ ^1P_1$, $(1s2p)\ ^3P_1$ ($E1$ transitions), decaying to the ground state $(1s1s)\ ^1S_0$. In the present work we apply the LPA for the derivation of all necessary formulas and develop it for the evaluation of transition probabilities for quasidegenerate levels in the framework of QED. In this paper we focus on the interelectron interaction corrections and leave the inclusion of the radiative corrections to subsequent studies.

Our paper is organized as follows. In Sec. II we present the general formulation of the LPA discussing its foundations and justification. A development of the LPA for the description of transition probabilities is presented in Sec. III. In Sec. III A we consider transition probabilities for one-electron ions. The next sections are devoted to two-electron ions. In Sec. III B the generic expressions for the transition probabilities in zeroth order (i.e., neglecting the interelectron interaction) are presented. The corresponding first-order expressions, where the one-photon exchange between the electrons is included, are given in Sec. III C. The formulas employed for the evaluation of amplitudes and transition probabilities are presented in Sec. IV. The formulas for the nondegenerate case (Sec. IV A) and for the degenerate case (Sec. IV B) are described separately. In Sec. IV C we derive the formulas for transition probabilities as they are applied in numerical calculations. Section V is devoted to the description of the com-

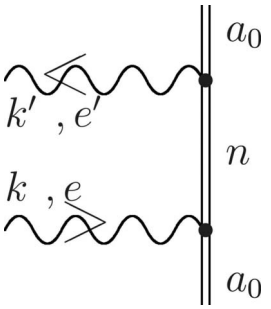

FIG. 1. Feynman graph, describing the photon scattering on an atomic electron. The wavy lines with the arrows describe the absorption and emission of photons with momenta k, k' and polarizations e, e', respectively. The double solid line denotes the electron in the field of the nucleus; a_0 corresponds to the ground electron state.

putational methods. The discussion and analysis of the results, their comparison with the other available data, and conclusions are found in Sec. VI.

II. LINE PROFILE APPROACH

The LPA is the version of QED PT which starts from the description of the atomic electrons as a set of noninteracting particles moving in the field of the nucleus $V^{\rm nuc}$ (Furry picture) and described by the solutions of the Dirac equation,

$$(\gamma_\mu \hat{p}^\mu - \gamma_0 V^{\rm nuc} - m)\psi = 0. \tag{1}$$

Here, $\hat{p}^\mu$ are the components of the momentum four vector, $p^0=\varepsilon$ is the bound-electron energy, and γ_μ are the conventional Dirac matrices. Throughout this paper we use the relativistic units where $\hbar=c=1$ and the fine-structure constant $\alpha=e^2/(\hbar c)$. The charge of the electron is $e=-|e|$. In this paper we designate the eigenvalues of Eq. (1) as ε while the physical one-electron energies as $\epsilon=\varepsilon+\Delta\epsilon$. The idea of the LPA is to evaluate the corrections to energy $(\Delta\epsilon)$ as the shift of position of resonance in some scattering process due to the interaction with the quantized electromagnetic field. This shift up to the very high orders of QED PT does not depend on the particular resonance process and when this dependence appears the concept of the energy level for the excited states cannot be strictly defined anymore [17]. For the practical implementation of the LPA the process of the elastic photon scattering on atomic electron was employed. This procedure in the lowest QED PT order is depicted in Fig. 1.

According to the standard Feynman rules (see, e.g., [24]), the S-matrix element for the graph depicted in Fig. 1 reads

$$S^{(2)} = (-ie)^2 \int d^4x_u d^4x_d \bar{\psi}_{a_0}(x_u)\gamma^{\mu_u} A_{\mu_u}^{(k',\lambda')*}(x_u) \times S(x_u,x_d)\gamma^{\mu_d} A_{\mu_d}^{(k,\lambda)}(x_d)\psi_{a_0}(x_d), \tag{2}$$

where $x^\mu=(t,\boldsymbol{r})$ denotes a space time point, $\psi_{a_0}(x) = \psi_{a_0}(\boldsymbol{r})e^{-i\varepsilon t}$ is the one-electron wave function, $\bar{\psi}=\psi^+\gamma^0$ is the Dirac conjugated wave function, $A_\mu^{(k,\lambda)}(x)=A_\mu^{(k,\lambda)}(\boldsymbol{r})e^{-i\omega t}$ is the four vector of the electromagnetic field potential (photon wave function), and $k^\mu=(\omega,\boldsymbol{k})$ and λ are the wave vector and polarization. The frequencies of the absorbed and emitted photons are $\omega=|\boldsymbol{k}|$ and $\omega'=|\boldsymbol{k}'|$, respectively. We employ the standard covariant notations for four vectors together with the sign convention for the metric tensor $(g_{\mu\nu})=\mathrm{diag}(1,-1,-1,-1)$. Einstein's sum convention is implied. The four-dimensional volume is $d^4x=dtd^3\boldsymbol{r}$.

We employ the notations x_u, x_d for the "up" and "down" vertex coordinates in Fig. 1. These nonstandard notations will be convenient for the more complicated graphs considered below. The bound-electron propagator is represented in terms of an eigenmode decomposition with respect to one-electron eigenstates of Eq. (1),

$$S(x_u,x_d) = \frac{i}{2\pi}\int d\omega_n e^{-i\omega(t_u-t_d)}\sum_n \frac{\psi_n(\boldsymbol{r}_u)\bar{\psi}_n(\boldsymbol{r}_d)}{\omega_n-\varepsilon_n(1-i0)}. \tag{3}$$

The sum over n runs over the entire Dirac spectrum. Note that the subscript at the integration variable (ω_n) is not the subject of summation over n. These indices are introduced again for the convenience in handling more complicated graphs.

Inserting the expressions for the propagator and wave functions in Eq. (2) and integrating over time and frequency variables we arrive at

$$S^{(2)} = (-2\pi i)\delta(\omega'-\omega)e^2\sum_n \frac{A_{a_0n}^{(k',\lambda')*}A_{na_0}^{(k,\lambda)}}{\omega+\varepsilon_{a_0}-\varepsilon_n}. \tag{4}$$

Here we employed the shorthand notation,

$$A_{ab}^{(k,\lambda)} = \int d^3\boldsymbol{r}\bar{\psi}_a(\boldsymbol{r})\gamma^\mu A_\mu^{(k,\lambda)}(\boldsymbol{r})\psi_b(\boldsymbol{r}). \tag{5}$$

The amplitude (U) of the process of elastic photon scattering is related to the S-matrix element via

$$S = (-2\pi i)\delta(\omega'-\omega)U, \tag{6}$$

where ω and ω' represent the energies of the initial and final states, respectively.

The resonance scattering means that the photon frequency ω is close to the energy difference between two atomic levels $\omega=\varepsilon_a-\varepsilon_{a_0}+O(\alpha)$, where α is the fine-structure constant. Accordingly, we have to retain only one term in the sum over n in Eq. (4). Then the resonance amplitude looks like

$$U^{(2)} = e^2\frac{A_{a_0a}^{(k',\lambda')*}A_{aa_0}^{(k,\lambda)}}{\omega+\varepsilon_{a_0}-\varepsilon_a}. \tag{7}$$

This amplitude has a singularity at $\omega=-\varepsilon_{a_0}+\varepsilon_a$. To avoid this singularity and to obtain the Lorentz profile for the photon absorption and photon emission processes we have to consider the radiative insertions into the internal electron line in Fig. 1. This insertion is depicted in Fig. 2.

The corresponding matrix element can be written down as

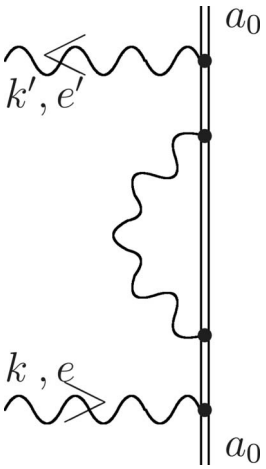

FIG. 2. Feynman graph corresponding to the electron self-energy insertion into the electron propagator in Fig. 1. The wavy line denotes the virtual photon. The other notations are the same as in Fig. 1.

$$S^{(4)} = (-ie)^4 \int d^4x_u d^4x_1 d^4x_2 d^4x_d \bar{\psi}_{a_0}(x_u)\gamma^{\mu_u} A^{(k',\lambda')*}_{\mu_u}(x_u) \times S(x_u,x_1)\gamma^{\mu_1} S(x_1,x_2)\gamma^{\mu_2} S(x_2,x_d)\gamma^{\mu_d} \times A^{(k,\lambda)}_{\mu_d}(x_d) D_{\mu_1\mu_2}(x_1,x_2)\psi_{a_0}(x_d), \quad (8)$$

where $D_{\mu_1\mu_2}(x_1,x_2)$ denotes the photon propagator which in the Feynman gauge reads

$$D_{\mu_1\mu_2}(x_1,x_2) = \frac{i}{2\pi}\int d\Omega I_{\mu_1\mu_2}(|\Omega|,r_{12}) e^{-i\Omega(t_1-t_2)}, \quad (9)$$

$$I_{\mu_1\mu_2}(\Omega,r_{12}) = g_{\mu_1\mu_2}\frac{1}{r_{12}} e^{i\Omega r_{12}}, \quad (10)$$

with $r_{12}=|\boldsymbol{r}_1-\boldsymbol{r}_2|$ and the metric tensor $g_{\mu_1\mu_2}$.

Integration over the time and frequency variables and employment of Eq. (6) lead to the following expression for the amplitude in the resonance approximation:

$$U^{(4)} = U^{(2)}\frac{\hat{\Sigma}_{aa}(\omega+\varepsilon_{a_0})}{\omega+\varepsilon_{a_0}-\varepsilon_a}. \quad (11)$$

Here we introduced the energy-dependent matrix element of the electron self-energy

$$\hat{\Sigma}_{ud}(\xi) = e^2 \sum_n \frac{i}{2\pi}\int d\Omega \frac{I_{unnd}(|\Omega|)}{\xi-\Omega-\varepsilon_n(1-i0)} \quad (12)$$

together with the shorthand notation

$$I_{u_1u_2d_1d_2}(\Omega) = \sum_{\mu_1\mu_2}\int d\boldsymbol{r}_1 d\boldsymbol{r}_2 \bar{\psi}_{u_1}(\boldsymbol{r}_1)\bar{\psi}_{u_2}(\boldsymbol{r}_2)\gamma^{\mu_1}\gamma^{\mu_2} \times I_{\mu_1\mu_2}(\Omega,r_{12})\psi_{d_1}(\boldsymbol{r}_1)\psi_{d_2}(\boldsymbol{r}_2). \quad (13)$$

It is assumed that the ultraviolet divergent matrix element (12) is renormalized in a standard way for the tightly bound electrons in atoms (see, e.g., [24]).

Repeating these insertions within the resonance approximation leads to the geometric progression. The resummation of this progression yields

$$U = e^2 \frac{A^{(k',\lambda')*}_{a_0a} A^{(k,\lambda)}_{aa_0}}{\omega+\varepsilon_{a_0}-V_a(\omega)}, \quad (14)$$

where

$$V_a(\omega) = V_a^{(0)} + \Delta V_a(\omega), \quad (15)$$

$$V_a^{(0)} = \varepsilon_a, \quad (16)$$

$$\Delta V_a(\omega) = \hat{\Sigma}_{aa}(\omega+\varepsilon_{a_0}). \quad (17)$$

Within the resonance approximation we can replace $\omega+\varepsilon_{a_0}$ by ε_a. Then $\Delta V_a=\hat{\Sigma}_{aa}(\varepsilon_a)$ represents the energy shift due to the lowest-order electron self-energy correction. It is convenient to decompose explicitly the electron self-energy matrix element into real and imaginary parts,

$$\hat{\Sigma}_{aa}(\varepsilon_a) = L_a - \frac{i}{2}\Gamma_a, \quad (18)$$

where L_a is the electron self-energy correction to the energy of the excited level a and Γ_a is the width of this level. Thus, the pole in Eq. (14) is shifted into the complex plane and the singularity on the real axis is avoided. The real parts of the resonance frequency in zeroth and first orders of PT are given by

$$\omega^{\mathrm{res},(0)} = -\varepsilon_{a_0}+\varepsilon_a, \quad (19)$$

$$\omega^{\mathrm{res},(0+1)} = -\varepsilon_{a_0}+\varepsilon_a+L_a. \quad (20)$$

Taking the amplitude [Eq. (14)] by square modulus, integrating over photon directions, and summing over photon polarizations we arrive at the probability (cross section) for the process of the photon scattering on a one-electron atom or ion. In the resonance approximation this probability factorizes into the product of absorption and emission probabilities with the same Lorentz-profile factor [17],

$$\mathcal{L}(\omega^{\mathrm{res}}) = \frac{\Gamma_{aa_0}}{(\omega-\omega^{\mathrm{res}})^2+\frac{1}{4}\Gamma_a^2}, \quad (21)$$

where Γ_{aa_0} is the partial width associated with the transition $a\to a_0$.

One of the most important problems within the LPA is the treatment of the ground state. An insertion of the electron self-energy correction into the outer electron lines in the standard Feynman graphs describing the elastic photon scattering on an atomic electron leads unavoidably to singularities. Since these outer lines correspond to the initial and final electron states, the problem of improving the energy of the ground state arises. Moreover the singularities leave the whole theory incomplete so far that the S matrix for the bound electrons actually does not exist. One way to circumvent these difficulties was suggested decades ago by Barbieri

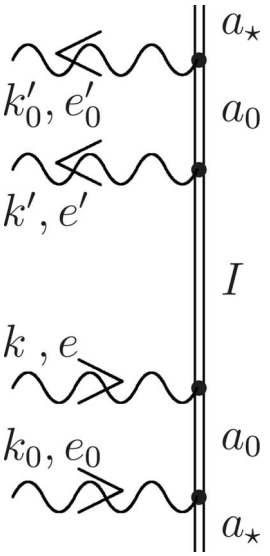

FIG. 3. The process of double-photon scattering on the artificial lower than ground state $a_\star$. Notations are the same as in Fig. 1.

and Sucher [53] whose idea was to evaluate the corrections to the transition probabilities via the imaginary part of the two-loop diagonal self-energy corrections for the ground state of an atom. Within the LPA we propose another solution of the problem [17,54]. To introduce the radiative corrections to the ground state we consider the more complicated two-photon process of the excitation of the resonant level a. This process starts from the one-photon absorption by an artificial "lower than ground" state $a_\star$ (see Fig. 3). This state plays the role of a regulator, which can be again removed at the end of evaluations. The insertions of the electron self-energy correction into the lower (or into the upper) electron propagator lead finally to the Lorentz line profile of the form [17,54]

$$\mathcal{L}(\omega^{\rm res}) = \frac{\Gamma_{aa_0} + \Gamma_{a_0 a_\star}}{(\omega - \omega^{\rm res})^2 + \frac{1}{4}(\Gamma_a + \Gamma_{a_0})^2} \tag{22}$$

in the emission process $a \to a_0 + \gamma$. In the most simple case of one channel decay the partial widths Γ_{aa_0}, $\Gamma_{a_0 a_\star}$ can be substituted by Γ_a, Γ_{a_0}, respectively. In Eq. (22) the integration over the second photon frequency ω_0 is performed and Γ_{a_0} represents the width of the level a_0. The presence of the width Γ_{a_0} is the only remnant of the introduced artificial lower than ground state $a_\star$. In Eq. (22) $\omega^{\rm res} = -\epsilon_{a_0} + \epsilon_a$ includes both corrections L_a to the energy ε_a and L_{a_0} to the energy ε_{a_0}. If both states a and a_0 are excited states, formula (22) represents the known expression for the Lorentz line shape in case of the decaying final state. In case of the ground a_0 state, we may consider Γ_{a_0} as the regulating parameter. Setting $\Gamma_{a_0} = 0$ at the end of the calculation, we obtain from Eq. (22) the emission line profile for the transition from the excited state a to the ground state a_0 with the radiative corrections for the ground state included in the definition of $\omega^{\rm res}$.

Now being able to evaluate any desired property of an atom including the ground-state energy corrections, we can disregard any insertions in the outer electron lines with their singularities and define the bound-electron S matrix in this way. Heuristically, this approach seems to be convincing, however, it looks unsatisfactory from the formal point of view. Therefore, we present a direct formal proof of the existence of the S matrix for the bound electrons based on the adiabatic approach. This proof was given earlier for the $S(\infty,0)$ matrix [55]. However, $S(\infty,0)$ matrix in QED provides difficulties with renormalization. Here we give the proof for $S(\infty,-\infty)$ matrix. Our starting point is the Sucher adiabatic $S_{\lambda_a}(\infty,-\infty)$ matrix [32] instead of Gell-Mann-Low adiabatic $S_{\lambda_a}(\infty,0)$ matrix [31] employed in [55].

The standard description of an arbitrary process in the free-electron QED starts from the time evolution of an initial state to a final state governed by the evolution operator within the interaction representation based on the relation

$$|\Phi(\infty)\rangle = T \exp\left\{ -i \int_{-\infty}^{\infty} dt \hat{H}^{\rm int}(t) \right\} |\Phi(-\infty)\rangle$$

$$= \hat{S}(\infty,-\infty)|\Phi(-\infty)\rangle. \tag{23}$$

Here, $\hat{H}^{\rm int}(t)$ is the interaction Hamiltonian in the interaction representation, $|\Phi(\pm\infty)\rangle$ are the state vectors at asymptotic times $t = \pm\infty$, and $\hat{S}(\infty,-\infty)$ is the evolution operator, usually called S matrix. The interaction between the particles involved is assumed to be absent at $t = \pm\infty$ and the transition probabilities due to the particle interactions at the finite time moments can be expressed in terms of matrix elements of S matrix.

Contrary to this, the interaction between the bound electrons is permanently present. Within the adiabatic formalism of Gell-Mann and Low [31] the interaction Hamiltonian $\hat{H}^{\rm int}(t)$ is replaced by the operator

$$\hat{H}^{\rm int}(t) = e^{-\lambda_a |t|} \hat{H}^{\rm int}(t), \tag{24}$$

where λ_a is the adiabatic parameter. Then, at the time moment $t = \pm\infty$ the interaction is switched off and at $t = 0$ is fully switched on. Using the interaction operator [Eq. (24)] one can perform the QED calculations in the usual manner and then set $\lambda_a = 0$ at the end, thus restoring the full interaction for the entire time intervals. This allows for the extension of the established techniques for calculating free-electron S-matrix elements to bound electrons in atoms.

Gell-Mann and Low [31] derived a formula which yields the energy shift of bound-electron states due to the interaction [Eq. (24)] in terms of the evolution operator $\hat{S}_{\lambda_a}(0,-\infty)$. Sucher [32] derived a symmetrized version of the energy shift formula, containing the matrix elements of the evolution operator $\hat{S}_{\lambda_a}(\infty,-\infty)$. On the basis of the Sucher formula an adiabatic S-matrix approach for the evaluation of the energy corrections in bound-electron QED was later developed [33].

Here we apply the adiabatic approach for another purpose. We will show that the singularities, arising after the electron self-energy insertions both in the initial and final

outer electron lines in the S-matrix element corresponding to the Feynman graph (Fig. 1), can be converted to the phase factor in the following way:

$$S_{\lambda_a} = (-2\pi i)\delta(\omega' - \omega)U \exp\left(\frac{\hat{\Sigma}_{a_0 a_0}(\varepsilon_{a_0})}{i\lambda_a}\right). \quad (25)$$

This is an asymptotic equation ($\lambda_a \to +0$). The λ_a dependence is located in the imaginary exponent. Here the amplitude U differs from Eqs. (6) and (7) by the replacement of ε_{a_0} to $\epsilon_{a_0}=\varepsilon_{a_0}+\hat{\Sigma}_{a_0 a_0}(\varepsilon_{a_0})$, where $\hat{\Sigma}_{a_0 a_0}(\varepsilon_{a_0})$ is the diagonal matrix element of the lowest-order electron self-energy operator. As for the ground state a_0 this matrix element is real, the phase factor does not contribute to the absolute value of amplitude defined by Eq. (6) and, accordingly, to the line profile. The proof is given in the Appendix. This proof can be repeated for any QED correction of any order. This result justifies the employment of the energy ϵ_{a_0} (with the QED corrections included) instead of ε_{a_0} in Eq. (14). The remaining finite contributions from all the insertions in the outer lines present the QED corrections to the outer wave functions. Moreover, this proof can be repeated also for the few-electron atoms. In this case the ground state will be corrected not only for the QED corrections but for the interelectron interaction as well. Thus, the problem of the existence of the bound-electron S matrix for the scattering process described by the Feynman graph (Fig. 1) is solved in any order of QED perturbation theory.

Now we go over to the most general formulation of the LPA. We will use the matrix formulation, which allows for the extension of the LPA to the case of quasidegenerate states. This formulation is also most suitable for the application of the LPA to the evaluation of transition probabilities. Within this formulation the generalization of Eq. (14) looks like

$$U = T^{+}\frac{1}{D(\omega)}T, \quad (26)$$

where the matrix T describes the absorption of the photon by the electron in the ground state a_0 with the excitation to the resonance (intermediate) state a. The matrix T^{+} describes the emission of the photon with the transition $a \to a_0$. The diagonal matrix (energy denominator) $D(\omega)$ is defined as

$$D(\omega) = \omega + \epsilon_{a_0} - V^{(0)}, \quad (27)$$

where ω is the photon frequency. The resonance condition reads

$$\omega^{\mathrm{res}} = -\epsilon_{a_0} + \varepsilon_a, \quad (28)$$

where ϵ_{a_0} is the energy of the ground state and ε_a is the Dirac energy of the state a. The energy ϵ_{a_0} is not necessarily equal to the Dirac energy; it may include already the radiative corrections (see discussion above). In Eq. (27) the diagonal matrix $D(\omega)$ involves

$$V^{(0)} = \varepsilon_a. \quad (29)$$

We employ here the matrix formulation of the single-photon scattering amplitude (26) on the one-electron ion in view of the further generalization of our approach to the quasidegenerate states in two-electron ions. This amplitude is described by the Feynman graph (Fig. 4). In this diagram we describe the photon interaction with the ground state by the boxes and deliberately omit the outer electron lines describing the ground-state wave functions. The justification of this approach was given above.

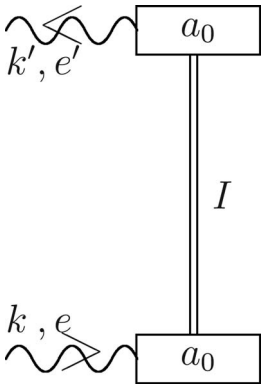

FIG. 4. The Feynman graph representing the process of elastic photon scattering on one-electron ion. The double solid line denotes the electron in the field of the nucleus (Furry picture of QED). The boxes with the wavy lines describe the absorption and emission of the photons by electron the ground state. The letter I at the internal electron line implies the resonance approximation, where only the resonant state I remains in the sum over the intermediate states in the electron propagator.

The next step is the insertion of the electron self-energy corrections in the internal electron line within the resonance approximation (see Fig. 5). The corresponding amplitude reads [47]

$$U = T^{+}\frac{1}{D(\omega)}\hat{\Sigma}(\omega + \epsilon_{a_0})\frac{1}{D(\omega)}T, \quad (30)$$

where $\hat{\Sigma}$ is the diagonal matrix corresponding to the regularized electron self-energy operator. In the case under consideration this matrix reduces to the diagonal matrix element of the electron self-energy operator for the state a.

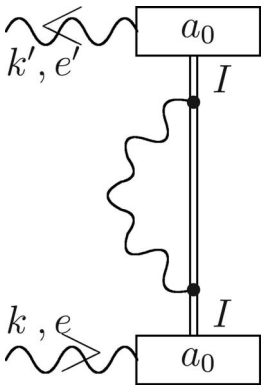

FIG. 5. The insertion of the one-loop electron self-energy in the internal electron line in Fig. 4. The wavy line describes the virtual photon. The other notations are the same as in Fig. 4.

Continuing recursively this process, i.e., inserting two, three, etc., self-energies in the internal electron line in Fig. 4 and summing the geometric progression, we obtain finally

$$U = T^{+}\frac{1}{D(\omega) - \Delta V(\omega)}T, \tag{31}$$

where $\Delta V(\omega)=\hat{\Sigma}(\omega+\epsilon_{a_0})$. Evaluation of the corresponding matrix element of the one-loop self-energy insertion at $\omega=\omega^{\mathrm{res}}$ leads back to Eq. (18).

Equation (31) illustrates the main idea of the LPA: the radiative corrections to the energy arise as the shifts of the resonance frequency due to the various insertions in the internal electron line in Fig. 4 in the resonance approximation. Graphically Eq. (31) can be represented by the Feynman graph (Fig. 6). Instead of the correction $\hat{\Sigma}$ in the box in graph (Fig. 6) any irreducible correction can be inserted; the corresponding energy shift will arise as the resonance frequency shift in Eq. (31).

In [45–47] the LPA was generalized to the few-electron ions, in particular for quasidegenerate states. The applications to two- and three-electron ions were presented. The general features of the LPA application to the evaluation of the transition probabilities were formulated in [17] and exemplified with some numerical studies.

In Sec. III of this paper we provide the detailed derivations of transition probabilities in the few-electron ions within the framework of the LPA.

III. TRANSITION PROBABILITIES

We are going to evaluate the transition probability for the process

$$I \overset{\omega_0}{\rightarrow} F, \tag{32}$$

where I is the initial two-electron state decaying to the final state F with emission of the photon ω_0. Within the framework of the LPA the state of an ion is associated with a position of the resonance. Therefore, we will consider a more general process which incorporates transition (32),

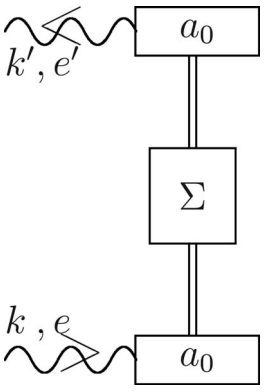

FIG. 6. The Feynman graph, illustrating Eq. (31). The box with the letter Σ inside corresponds to the infinite number of successive insertions of the type (Fig. 5).

$$A_0 \overset{\omega}{\rightarrow} I \overset{\omega_0}{\rightarrow} F \overset{\omega'}{\rightarrow} A_0, \tag{33}$$

i.e., a transition from the state A_0 (let A_0 be the ground state) to the state I with absorption of a photon ω. Then, the state I decays to the state F with emission of the photon ω_0 and, finally, the state F decays back to the state A_0 with emission of a photon ω'. The initial state (I) is associated with the resonance near $\omega=-E_{A_0}+E_I^{(0)}$, where $E_I^{(0)}$ is the zero-order energy of the state I (sum of the Dirac energies). The final state (F) is defined by the resonance near $\omega'=-E_{A_0}+E_F^{(0)}$. The energy of the ground state A_0 is given by E_{A_0}.

It will be shown below that in the resonance approximation the amplitude of scattering process (33) can be written as

$$U = T^{+}\frac{1}{D(\omega') - \Delta V(\omega')}\Xi(\omega_0)\frac{1}{D(\omega) - \Delta V(\omega)}T. \tag{34}$$

The matrix T describes the absorption of the photon ω by the ground state A_0; the matrix T^{+} describes the emission of the photon ω' with the transition to the ground state A_0. The matrix $D(\omega)$ is defined by Eq. (27), where $V^{(0)}$ is now the sum of the Dirac energies for the electrons which belong to the state I. The matrix D is diagonal in the basis of the two-electron functions in the j-j coupling scheme. The matrix of the interaction operator $\Delta V(\omega)$ was investigated in [47]. Here we will construct it in the first order of the perturbation theory.

The right denominator corresponds to the resonance associated with the state I and the left one defines the resonance for the state F. The function $\Xi(\omega_0)$ is a complicated vertex which describes the emission of photon ω_0 by the ion in the state I decaying to the state F. The matrix element of the vertex $\Xi(\omega_0)$ calculated on the eigenvectors Φ_I and Φ_F of the matrices $D(\omega)-\Delta V(\omega)$ and $D(\omega')-\Delta V(\omega')$ corresponding to the states I and F, respectively, represents the amplitude of the decay process (32),

$$U_{I\rightarrow F} = (\Xi(\omega_0))_{\Phi_F\Phi_I}. \tag{35}$$

The eigenvectors Φ_I and Φ_F and the vertex $\Xi(\omega_0)$ can be constructed order by order employing perturbation theory. This procedure is formulated consistently in Secs. III A–III C.

Below in this section we will derive general formulas for the transition probabilities in two-electron ions in zeroth and first orders of the QED perturbation theory considering the interelectron interaction as perturbation.

A. One-electron ion

In order to introduce our notations we start from the one-photon transition in a one-electron ion within zeroth-order QED perturbation theory. This process with transition from

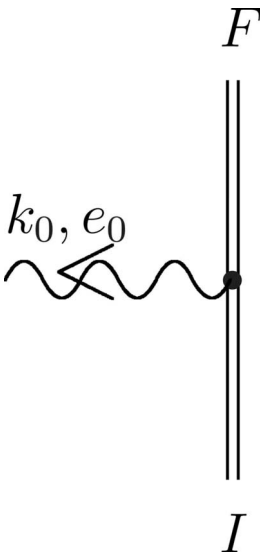

FIG. 7. The Feynman graph representing the process of the photon emission. The labels I and F correspond to the initial and final states.

the initial state I into the final state F is described by Eq. (32).

In zeroth-order QED perturbation theory the corresponding S-matrix element is given by Feynman graph depicted in Fig. 7 and reads

$$S = \int d^4x \bar{\psi}_F(\boldsymbol{r}) e^{it\varepsilon_F}(-ie)\gamma^\mu A_\mu^{(k_0,\lambda_0)*}(\boldsymbol{r}) e^{i\omega_0 t} e^{-it\varepsilon_I}\psi_I(\boldsymbol{r}). \tag{36}$$

The Dirac functions $\psi_I(\boldsymbol{r})$, $\bar{\psi}_F(\boldsymbol{r})$ and the Dirac energies ε_I, ε_F characterize the initial and final one-electron states. The emitted photon is described by the momentum four vector k_0 and the polarization λ_0.

In the coordinate representation the photon wave function,

$$A^{\mu(k,\lambda)}(\boldsymbol{r})e^{-i\omega t} = \sqrt{\frac{2\pi}{\omega}}\epsilon^{\mu(\lambda)}e^{-i(\omega t - \boldsymbol{kr})}, \quad \mu = 1,2,3, \tag{37}$$

describes a photon with the momentum k and polarization λ ($\epsilon^{(\lambda)}$ is the polarization four vector). Here, the photon wave function is understood within the "transverse" gauge, which in the work [50] is referred as the "velocity" gauge,

$$A^{0(k,\lambda)}(\boldsymbol{r})e^{-i\omega t} = 0. \tag{38}$$

Performing the integration over the time variable yields

$$S = (-2\pi i)\delta(\varepsilon_F + \omega_0 - \varepsilon_I)e\int d^3\boldsymbol{r}\bar{\psi}_F(\boldsymbol{r})\gamma^\mu A_\mu^{(k_0,\lambda_0)*}(\boldsymbol{r})\psi_I(\boldsymbol{r}). \tag{39}$$

The expression for the amplitude (U) of the process is defined by Eq. (6). Then, the amplitude corresponding to Eq. (39) reads

$$U = e\int d^3\boldsymbol{r}\bar{\psi}_F(\boldsymbol{r})\gamma^\mu A_\mu^{(k_0,\lambda_0)*}(\boldsymbol{r})\psi_I(\boldsymbol{r}). \tag{40}$$

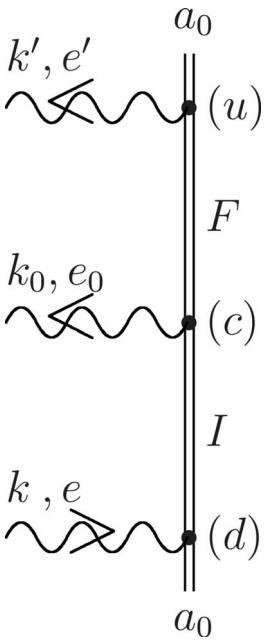

FIG. 8. The Feynman graphs representing the process of photon emission in the LPA. This graph incorporates the graph in Fig. 7. The upper, central, and down vertices are specified by corresponding subscripts (u), (c), and (d), respectively.

Within the framework of the line profile approach we consider a process described by Eq. (33). This process is depicted in Fig. 8. The S-matrix element corresponding to Fig. 8 is written as

$$\begin{aligned} S = \int d^4x_u d^4x_c d^4x_d d\omega_u d\omega_d \bar{\psi}_{a_0}(\boldsymbol{r}_u) e^{it_u(\varepsilon_{a_0})}(-ie) \\ \times \gamma^{\mu_u} A_{\mu_u}^{(k',\lambda')*}(\boldsymbol{r}_u) e^{i\omega' t_u}\frac{i}{2\pi} \\ \times \sum_u \frac{\psi_u(\boldsymbol{r}_u)\bar{\psi}_u(\boldsymbol{r}_c)}{\omega_u - \varepsilon_u(1-i0)} e^{-i\omega_u(t_u - t_c)} \\ \times (-ie)\gamma^{\mu_c} A_{\mu_c}^{(k_0,\lambda_0)*}(\boldsymbol{r}_c) e^{i\omega_0 t_c}\frac{i}{2\pi} \\ \times \sum_d \frac{\psi_d(\boldsymbol{r}_c)\bar{\psi}_d(\boldsymbol{r}_d)}{\omega_d - \varepsilon_d(1-i0)} e^{-i\omega_d(t_c - t_d)}(-ie)\gamma^{\mu_d} \\ \times A_{\mu_d}^{(k,\lambda)}(\boldsymbol{r}_d) e^{-i\omega t_d} e^{-it_d(\varepsilon_{a_0})}\psi_{a_0}(\boldsymbol{r}_d). \end{aligned} \tag{41}$$

We employ notations u, c, and d for the upper, central, and lower vertices of Feynman graphs. Note that subscripts at the integration variables ω_u, ω_d refer to the corresponding vertices. After integration over the time variables and over the frequencies (ω_u, ω_d) we get the expression defining the amplitude (U) of the scattering process,

$$S=(-2\pi i)\delta(\omega'+\omega_0-\omega)e^3\int d^3\boldsymbol{r}_u d^3\boldsymbol{r}_c d^3\boldsymbol{r}_d \bar{\psi}_{a_0}(\boldsymbol{r}_u)\gamma^{\mu_u}A^{(k',\lambda')*}_{\mu_u}(\boldsymbol{r}_u)\sum_u \frac{\psi_u(\boldsymbol{r}_u)\bar{\psi}_u(\boldsymbol{r}_c)}{\varepsilon_{a_0}+\omega'-\varepsilon_u}$$

$$\times\gamma^{\mu_c}A^{(k_0,\lambda_0)*}_{\mu_c}(\boldsymbol{r}_c)\sum_d \frac{\psi_d(\boldsymbol{r}_c)\bar{\psi}_d(\boldsymbol{r}_d)}{\varepsilon_{a_0}+\omega-\varepsilon_d}\gamma^{\mu_d}A^{(k,\lambda)}_{\mu_d}(\boldsymbol{r}_d)\psi_{a_0}(\boldsymbol{r}_d) \tag{42}$$

$$=(-2\pi i)\delta(\omega'+\omega_0-\omega)U. \tag{43}$$

Being interested in the transition between I and F states we consider the frequencies of the absorbed and emitted photons satisfying the conditions

$$\omega=-\varepsilon_{a_0}+\varepsilon_I+\mathrm{O}(\alpha), \tag{44}$$

$$\omega'=-\varepsilon_{a_0}+\varepsilon_F+\mathrm{O}(\alpha). \tag{45}$$

Let us also assume that the states I, F are well isolated. Hence, we can rewrite the amplitude in Eq. (43) as

$$U=e^3\int d^3\boldsymbol{r}_u d^3\boldsymbol{r}_c d^3\boldsymbol{r}_d \bar{\psi}_{a_0}(\boldsymbol{r}_u)\gamma^{\mu_u}A^{(k',\lambda')*}_{\mu_u}(\boldsymbol{r}_u)\frac{\psi_F(\boldsymbol{r}_u)\bar{\psi}_F(\boldsymbol{r}_c)}{\varepsilon_{a_0}+\omega'-\varepsilon_F}$$

$$\times\gamma^{\mu_c}A^{(k_0,\lambda_0)*}_{\mu_c}(\boldsymbol{r}_c)\frac{\psi_I(\boldsymbol{r}_c)\bar{\psi}_I(\boldsymbol{r}_d)}{\varepsilon_{a_0}+\omega-\varepsilon_I}\gamma^{\mu_d}A^{(k,\lambda)}_{\mu_d}(\boldsymbol{r}_d)\psi_{a_0}(\boldsymbol{r}_d)+R, \tag{46}$$

where R denotes the terms regular at ω, ω' given by Eqs. (44) and (45). The first term is singular and it defines the resonances corresponding to the initial state I and to the final state F. In the resonance approximation we retain only the terms singular at the positions of resonances which means that we neglect the terms denoted by R. The corresponding corrections are called nonresonant corrections. These corrections give rise to an asymmetry of the line profile and define the level of accuracy at which the concept of energy levels itself becomes inadequate for the analysis of experimental data. They are investigated in [56,57] for highly charged ions and in [58–64] for the hydrogen atom.

Aiming for the application of the LPA to two-electron ions we introduce the following notations. The vertex functions Φ_{a_0}, $\Phi^+_{a_0}$ representing absorption of the photon by the electron in the state a_0 and emission of the photon with subsequent decay of an atom into the state a_0, respectively, are

$$\Phi_{a_0}(\boldsymbol{r})=e\gamma^{\mu}A^{(k,\lambda)}_{\mu}(\boldsymbol{r})\psi_{a_0}(\boldsymbol{r}), \tag{47}$$

$$\Phi^+_{a_0}(\boldsymbol{r})=e\bar{\psi}_{a_0}(\boldsymbol{r})\gamma^{\mu}A^{(k',\lambda')*}_{\mu}(\boldsymbol{r}). \tag{48}$$

Then, the expression for the amplitude takes the form

$$U=e\int d^3\boldsymbol{r}_u d^3\boldsymbol{r}_c d^3\boldsymbol{r}_d \Phi^+_{a_0}(\boldsymbol{r}_u)\frac{\psi_F(\boldsymbol{r}_u)\bar{\psi}_F(\boldsymbol{r}_c)}{\varepsilon_{a_0}+\omega'-\varepsilon_F}$$

$$\times\gamma^{\mu_c}A^{(k_0,\lambda_0)*}_{\mu_c}(\boldsymbol{r}_c)\frac{\psi_I(\boldsymbol{r}_c)\bar{\psi}_I(\boldsymbol{r}_d)}{\varepsilon_{a_0}+\omega-\varepsilon_I}\Phi_{a_0}(\boldsymbol{r}_d)+R. \tag{49}$$

Introducing notations

$$T_{na_0}=-\int d^3\boldsymbol{r}\bar{\psi}_n(\boldsymbol{r})\Phi_{a_0}(\boldsymbol{r}), \tag{50}$$

$$T^+_{a_0n}=-\int d^3\boldsymbol{r}\Phi^+_{a_0}(\boldsymbol{r})\psi_n(\boldsymbol{r}) \tag{51}$$

we can reexpress Eq. (46) as

$$U=T^+_{a_0F}\frac{1}{\varepsilon_{a_0}+\omega'-\varepsilon_F}e\int d^3\boldsymbol{r}\bar{\psi}_F(\boldsymbol{r})\gamma^{\mu}A^{(k_0,\lambda_0)*}_{\mu}(\boldsymbol{r})\psi_I(\boldsymbol{r})$$

$$\times\frac{1}{\varepsilon_{a_0}+\omega-\varepsilon_I}T_{Ia_0}+R. \tag{52}$$

Introducing the matrices

$$\Xi_{n_1n_2}(\omega_0)=e\int d^3\boldsymbol{r}\bar{\psi}_{n_1}(\boldsymbol{r})\gamma^{\mu}A^{(k_0,\lambda_0)*}_{\mu}(\boldsymbol{r})\psi_{n_2}(\boldsymbol{r}), \tag{53}$$

$$D_{n_1n_2}(\omega)=(\omega+\varepsilon_{a_0}-\varepsilon_{n_1})\delta_{n_1,n_2}, \tag{54}$$

where δ_{n_1,n_2} means the Kronecker symbol, we can write the expression for the amplitude in matrix form,

$$U=T^+_{a_0}D^{-1}(\omega')\Xi(\omega_0)D^{-1}(\omega)T_{a_0} \tag{55}$$

$$=T^+_{a_0}\frac{1}{D(\omega')}\Xi(\omega_0)\frac{1}{D(\omega)}T_{a_0}. \tag{56}$$

Expression (56) coincide with Eq. (34) in zeroth order: $\Delta V=0+\mathrm{O}(\alpha)$. Taking into account the radiative corrections, the matrix ΔV will contain radiative insertions such as the self-energy and vacuum-polarization operators. As it was mentioned above in the present studies we will neglect the influence of the radiative corrections.

According to Eq. (35) the amplitude of the process described by Eq. (32) reads in the zeroth order of the perturbation theory

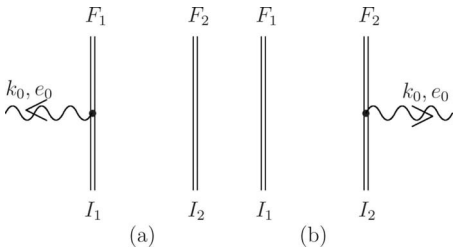

FIG. 9. The Feynman graphs representing the single-photon transition in a two-electron ion to lowest order in α. The notations are the same as in Figs. 4–8. I_i $(i=1,2)$ and F_i $(i=1,2)$ denote the initial and final states for the two electrons.

$$U = (\Xi)_{FI}. \tag{57}$$

As the matrix $D(\omega)$ is diagonal on the Dirac functions and $\Delta V=0$, the Dirac functions corresponding to the initial state I and to the final state F are the eigenvectors for the matrices $D(\omega)-\Delta V(\omega)$ and $D(\omega')-\Delta V(\omega')$, respectively.

As a consequence of the application of the resonance approximation amplitude Eq. (57) does not depend on the particular choice for the functions Φ_{a_0}, $\Phi^+_{a_0}$, which means that amplitude (57) does not depend on how the initial state I was excited and how the final state F decayed. Accordingly, the state a_0 can be an arbitrary state. In the further derivations we will chose states Φ_{a_0}, $\Phi^+_{a_0}$ calculated within lowest orders of the perturbation theory.

B. Two-electron ions: Zeroth-order perturbation theory

In the zeroth order of the QED perturbation theory the S-matrix element for the process [Eq. (32)] in two-electron ions is given by the Feynman graphs (Fig. 9). Within the framework of the line profile approach we consider process given by Eq. (33). We assume the state A_0 as being the ground state.

In the approximation of noninteracting electrons the S-matrix element corresponding to scattering process (33) is given by the Feynman graphs in Fig. 10. Graphs (a) and (b) yield the same contribution, so we will consider twice the graph [Fig. 10(a)].

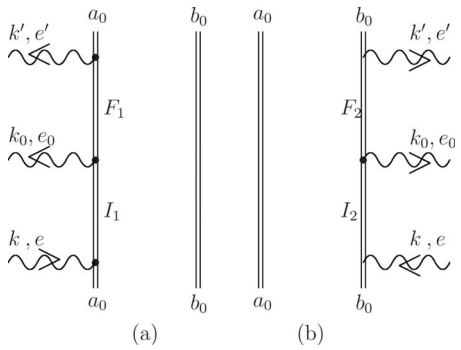

FIG. 10. The Feynman graphs representing the process of elastic photon scattering on the two-electron ion within the LPA. These graphs incorporate the graphs in Fig. 9. See in the text the notations a_0, b_0.

In zeroth order the wave function of the ground state can be taken as Slater determinant,

$$\Psi^{(0)}_{A_0}(x_1,x_2) = \frac{1}{\sqrt{2}}\det\{\psi_{a_0}(x_1)\psi_{b_0}(x_2)\} = \Psi^{(0)}_{A_0}(\boldsymbol{r}_1,\boldsymbol{r}_2)e^{-i\varepsilon_{1s}(t_1+t_2)}. \tag{58}$$

Here, $\psi_{a_0}(x)=\psi_{1s+}(x)=\psi_{1s+}(\boldsymbol{r})e^{-i\varepsilon_{1s}t}$, $\psi_{b_0}(x)=\psi_{1s-}(x)$ refer to Dirac one-electron functions with different projections of the total one-electron angular momentum (identical with electron spin in case of first state). In zeroth order the ground-state energy (E_{A_0}) is $E^{(0)}_{A_0}=2\varepsilon_{1s}$. The S-matrix element represented by the diagrams in Fig. 10 is the same as the S-matrix element represented by Fig. 8 and, accordingly, it is given by Eq. (41).

With the purpose of employment of the matrix $\Xi(\omega_0)$ introduced in Eq. (34) we rewrite the S-matrix element corresponding to the Feynman graph [Fig. 10(a)] in the form

$$\begin{aligned} S = (-i)^2 \int & d^4x_{u_1} d^4x_{u_2} d^4x_{c_1} d^4x_{d_1} d^4x_{d_2} d\omega_{u_1} d\omega_{d_1} d\omega_n \bar{\Phi}^{(0)}_{A_0}(\boldsymbol{r}_{u_1},\boldsymbol{r}_{u_2}) e^{it_{u_1}(E^{(0)}_{A_0}+\omega')} \delta(t_{u_1}-t_{u_2}) \\ & \times \frac{i}{2\pi}\sum_{u_1} \frac{\psi_{u_1}(\boldsymbol{r}_{u_1})\bar{\psi}_{u_1}(\boldsymbol{r}_{c_1})}{\omega_{u_1}-\varepsilon_{u_1}(1-i0)} e^{-i\omega_{u_1}(t_{u_1}-t_{c_1})}(-ie)\gamma^{\mu_{c_1}} A^{(k_0,\lambda_0)*}_{\mu_{c_1}}(\boldsymbol{r}_{c_1}) e^{i\omega_0 t_{c_1}} \frac{i}{2\pi}\sum_{d_1} \frac{\psi_{d_1}(\boldsymbol{r}_{c_1})\bar{\psi}_{d_1}(\boldsymbol{r}_{d_1})}{\omega_{d_1}-\varepsilon_{d_1}(1-i0)} e^{-i\omega_{d_1}(t_{c_1}-t_{d_1})} \\ & \times \frac{i}{2\pi}\sum_{n} \frac{\psi_n(\boldsymbol{r}_{u_2})\bar{\psi}_n(\boldsymbol{r}_{d_2})}{\omega_n-\varepsilon_n(1-i0)} e^{-i\omega_n(t_{u_2}-t_{d_2})} e^{-it_{d_1}(E^{(0)}_{A_0}+\omega)} \delta(t_{d_1}-t_{d_2}) \Phi^{(0)}_{A_0}(\boldsymbol{r}_{d_1},\boldsymbol{r}_{d_2}), \end{aligned} \tag{59}$$

where we have introduced the two-electron vertex functions,

$$\Phi^{(0)}_{A_0}(\boldsymbol{r}_1,\boldsymbol{r}_2) = e\gamma^\mu A^{(k,\lambda)}_\mu(\boldsymbol{r}_1)\Psi^{(0)}_{A_0}(\boldsymbol{r}_1,\boldsymbol{r}_2), \tag{60}$$

$$\bar{\Phi}^{(0)}_{A_0}(\boldsymbol{r}_1,\boldsymbol{r}_2) = \bar{\Psi}^{(0)}_{A_0}(\boldsymbol{r}_1,\boldsymbol{r}_2)e\gamma^\mu A^{*(k',\lambda')}_\mu(\boldsymbol{r}_1), \tag{61}$$

and function conjugated to function (58),

$$\bar{\Psi}^{(0)}_{A_0}(x_1,x_2)=\frac{1}{\sqrt{2}}\det\{\bar{\psi}_{a_0}(x_1)\bar{\psi}_{b_0}(x_2)\}=\bar{\Psi}^{(0)}_{A_0}(\boldsymbol{r}_1,\boldsymbol{r}_2)e^{i\varepsilon_{1s}(t_1+t_2)}. \tag{62}$$

As in the case of the one-electron ion the functions $\Phi^{(0)}_{A_0}$, $\bar{\Phi}^{(0)}_{A_0}$ describe the properties of the scattering process [compare Eqs. (47) and (48)].

The S-matrix element, corresponding to the Feynman graph [Fig. 10(a)], contains two-electron propagators. In Eq. (59) we formally introduced the third propagator $S(x_{u_2},x_{d_2})$. We have to show that expression (59) leads to Eq. (42). With the aid of the Dirac-Sokhotsky formulas we can write

$$[\omega_n-\varepsilon_n(1-i0)]^{-1}=\frac{2\pi}{i}\delta(\omega_n-\varepsilon_n)-[-\omega_n+\varepsilon_n+i0\varepsilon_n)^{-1}. \tag{63}$$

Employing this identity and integrating over variables t_{u_2}, t_{d_2} and ω_n, because of orthogonality of the Dirac functions, reduces the sum over n to terms $n=1s$ only. The first term in the right-hand side of Eq. (63) yields Eq. (42), while the second term vanishes after integration over ω_{u_1} (because $\varepsilon_n>0$ and the both poles lie in the same complex half plane).

Going beyond the approximation of noninteracting electrons, the functions Φ_{A_0}, $\bar{\Phi}_{A_0}$ will be more complicated functions than Slater determinants [Eqs. (60) and (61)]. However, when calculating transition probability we can ignore the details involved in the preparation of the initial state (I) and the further decay of the final state (F). Accordingly, in the resonance approximation, there is no need to specify the functions Φ_{A_0}, $\bar{\Phi}_{A_0}$.

In order to utilize efficiently the Feynman graphs, technique within the framework of the line profile approach in the case of the two-electron ions, we introduced two elements: lower and upper boxes with letters A_0 inside. These boxes describe the two-electron state A_0 absorbing or emitting a photon. These lower and upper boxes correspond to the following expressions in the S-matrix elements [see Eq. (59)]:

$$e^{-it_{d_1}(E_{A_0}+\omega)}\delta(t_{d_1}-t_{d_2})\Phi_{A_0}(\boldsymbol{r}_{d_1},\boldsymbol{r}_{d_2}),$$

$$\bar{\Phi}_{A_0}(\boldsymbol{r}_{u_1},\boldsymbol{r}_{u_2})e^{it_{u_1}(E_{A_0}+\omega')}\delta(t_{u_1}-t_{u_2}),$$

respectively. Accordingly, in zeroth order of the perturbation theory the S-matrix element for the scattering process [Eq. (33)] is represented by the graphs in Fig. 11 and is given by Eq. (59).

Integration over the time variables in Eq. (59) yields the following expression:

$$\begin{aligned}S=(-i)^3\left(\frac{i}{2\pi}\right)^3(2\pi)^3\sum_{u_1d_1n}\int d\omega_{u_1}d\omega_{d_1}d\omega_n\Delta_{65}\\ \times T^{+}_{A_0u_1n}e(A^{(k_0,\lambda_0)*})_{u_1d_1}T_{d_1nA_0}[\omega_{u_1}-\varepsilon_{u_1}(1-i0)]^{-1}\\ \times[\omega_{d_1}-\varepsilon_{d_1}(1-i0)]^{-1}[\omega_n-\varepsilon_n(1-i0)]^{-1},\end{aligned} \tag{64}$$

which involves the following shorthand notations:

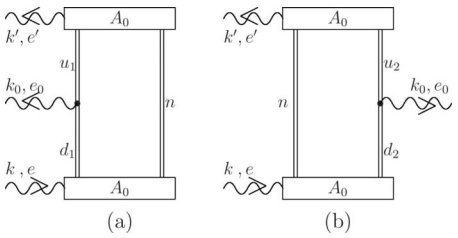

FIG. 11. The Feynman graphs representing the process of elastic photon scattering on the two-electron ion. The boxes with the letter A_0 inside and wavy lines depict complicated vertices describing the absorption and emission of a photon by the two-electron ion. The photon line in the center denotes the emission of a photon with frequency $\omega_0=|\boldsymbol{k}_0|$ corresponding to the transition energy from the initial to the final two-electron state.

$$\begin{aligned}\Delta_{65}=\delta(E_{A_0}+\omega'-\omega_{u_1}-\omega_n)\delta(\omega_{u_1}-\omega_{d_1}+\omega_0)\\ \times\delta(\omega_{d_1}+\omega_n-E_{A_0}-\omega),\end{aligned} \tag{65}$$

the complicated vertex

$$T_{n_1n_2A_0}=-\int d^3\boldsymbol{r}_1d^3\boldsymbol{r}_2\bar{\psi}_{n_1}(\boldsymbol{r}_1)\bar{\psi}_{n_2}(\boldsymbol{r}_2)\Phi_{A_0}(\boldsymbol{r}_1,\boldsymbol{r}_2) \tag{66}$$

and the one-electron matrix element

$$A^{(k,\lambda)}_{n_1n_2}=\int d^3\boldsymbol{r}\bar{\psi}_{n_1}(\boldsymbol{r})\gamma^\mu A^{(k,\lambda)}_\mu(\boldsymbol{r})\psi_{n_2}(\boldsymbol{r}). \tag{67}$$

We are interested in the transition probability at the frequencies corresponding to the positions of resonances

$$\omega=-E_{A_0}+E^{(0)}_I+O(\alpha), \tag{68}$$

$$\omega'=-E_{A_0}+E^{(0)}_F+O(\alpha). \tag{69}$$

To zeroth order $E^{(0)}_I=\varepsilon_{I_1}+\varepsilon_{I_2}$ and $E^{(0)}_F=\varepsilon_{F_1}+\varepsilon_{F_2}$ determine the positions of the resonances (sum of the Dirac energies) corresponding to the initial and final states, respectively. Within the framework of the resonance approximation one can retain only the terms which are singular at the positions of resonances. The Dirac energies ε_{I_1}, ε_{I_2}, ε_{F_1}, and ε_{F_2} correspond to the positive-energy electron states; accordingly, within the resonance approximation we can omit all terms $\varepsilon_{u_1}<0$, $\varepsilon_{d_1}<0$, and $\varepsilon_n<0$, which fixes the signs of the imaginary part of the poles in Eq. (64).

Applying Eq. (63) we can write the following equality:

$$\begin{aligned}&\Delta_{65}[\omega_{u_1}-\varepsilon_{u_1}(1-i0)]^{-1}[\omega_{d_1}-\varepsilon_{d_1}(1-i0)]^{-1}\\ &\quad\times[\omega_n-\varepsilon_n(1-i0)]^{-1}\\ &\quad=\Delta_{65}[E_{A_0}+\omega'-\varepsilon_{u_1}-\varepsilon_n]^{-1}[E_{A_0}+\omega-\varepsilon_{d_1}-\varepsilon_n]^{-1}\\ &\qquad\times\frac{2\pi}{i}\delta(E_{A_0}+\omega-\omega_{d_1}-\varepsilon_n)+\Delta_{65}R.\end{aligned} \tag{70}$$

The abbreviation $\Delta_{65}R$ for the product between Δ_{65} as given by Eq. (65) and the quantity R referring exclusively to the terms which are regular at the positions of the resonances is

employed. These terms are regular because the imaginary parts of the poles enter with equal signs.

We employ Eq. (70) for the evaluation of Eq. (64). Moreover, applying the resonance approximation in Eq. (64) all the regular terms R in Eq. (70) can be omitted and the sum over u_1, d_1, n reduces to the terms only, which satisfy the conditions

$$\varepsilon_{d_1} + \varepsilon_n = E_I^{(0)} = \varepsilon_{I_1} + \varepsilon_{I_2}, \tag{71}$$

$$\varepsilon_{u_1} + \varepsilon_n = E_F^{(0)} = \varepsilon_{F_1} + \varepsilon_{F_2}. \tag{72}$$

Accordingly, for the contribution of the Feynman graph [Fig. 11(a)] we can write

$$S^{\mathrm{l}} = (-2\pi i)\delta(\omega - \omega_0 - \omega') \times T^{+}_{A_0 u_1 n}[E_{A_0} + \omega' - \varepsilon_{u_1} - \varepsilon_n]^{-1} e A^{(k_0,\lambda_0)*}_{u_1 d_1} \times [E_{A_0} + \omega - \varepsilon_{d_1} - \varepsilon_n]^{-1} T_{d_1 n A_0}. \tag{73}$$

Here, we suppose that u_1, d_1, n match with the conditions [Eqs. (71) and (72)], so that the index d_1 runs over I_1, I_2, index u_1 runs over F_1, F_2, and index n runs over I_1, I_2, F_1, F_2. This yields a nonvanishing contribution only if $I_2 = F_2$ (single excitation).

In the same way the expression for S-matrix element corresponding to graph [Fig. 11(b)] can be derived,

$$S^{\mathrm{r}} = (-2\pi i)\delta(\omega - \omega_0 - \omega') T^{+}_{A_0 n u_2}[E_{A_0} + \omega' - \varepsilon_n - \varepsilon_{u_2}]^{-1} \times e A^{(k_0,\lambda_0)*}_{u_2 d_2}[E_{A_0} + \omega - \varepsilon_n - \varepsilon_{d_2}]^{-1} T_{n d_2 A_0}, \tag{74}$$

where the states u_2, d_2, n now satisfy the conditions

$$\varepsilon_n + \varepsilon_{d_2} = E_I^{(0)}, \tag{75}$$

$$\varepsilon_n + \varepsilon_{u_2} = E_F^{(0)}. \tag{76}$$

One can verify that the results for the graphs [Figs. 11(a) and 11(b)] are equal, i.e.,

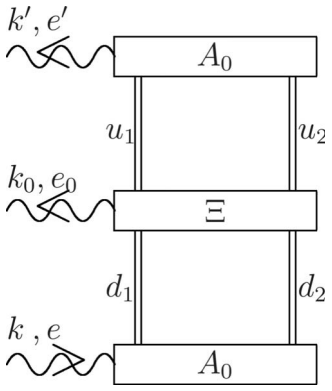

FIG. 12. The Feynman graph representing the process of elastic photon scattering on the two-electron ion. In addition to Fig. 11 the box with letter Ξ inside and with an external photon indicates the complicated vertex for the emission of a photon ω_0 corresponding to the transition from the initial to the final state $(I \to F)$.

$$S^l = S^r. \tag{77}$$

Our goal is to present expressions [Eqs. (73) and (74)] in the form of Eq. (34). In doing so, we consider the graph depicted on Fig. 12. The block Ξ represents a complicated vertex describing the emission of the photon ω_0. This vertex can be written in the form

$$\Xi(x_{c_1}, x_{c_2}, x_{s_1}, x_{s_2}) = \Xi(\boldsymbol{r}_{c_1}, \boldsymbol{r}_{c_2}, \boldsymbol{r}_{s_1}, \boldsymbol{r}_{s_2}) e^{i t_{c_1} \omega_0} \delta(t_{c_2} - t_{c_1}) \times \delta(t_{s_1} - t_{c_1}) \delta(t_{s_2} - t_{c_1}). \tag{78}$$

The function Ξ is a generic but yet unknown function. It can be derived under the requirement that the graph in Fig. 12 yields the same contribution as the graphs in Fig. 11. The S matrix corresponding to Fig. 12 appears as

$$S = (-i)^2 \int d^4x_{u_1} d^4x_{u_2} d^4x_{c_1} d^4x_{c_2} d^4x_{s_1} d^4x_{s_2} d^4x_{d_1} d^4x_{d_2} d\omega_{u_1} d\omega_{u_2} d\omega_{d_1} d\omega_{d_2} \bar{\Phi}_{A_0}(\boldsymbol{r}_{u_1}, \boldsymbol{r}_{u_2}) e^{i t_{u_1}(E_{A_0} + \omega')} \delta(t_{u_1} - t_{u_2}) \times \frac{i}{2\pi} \sum_{u_1} \frac{\psi_{u_1}(\boldsymbol{r}_{u_1}) \bar{\psi}_{u_1}(\boldsymbol{r}_{c_1})}{\omega_{u_1} - \varepsilon_{u_1}(1 - i0)} e^{-i\omega_{u_1}(t_{u_1} - t_{c_1})} \frac{i}{2\pi} \sum_{u_2} \frac{\psi_{u_2}(\boldsymbol{r}_{u_2}) \bar{\psi}_{u_2}(\boldsymbol{r}_{c_2})}{\omega_{u_2} - \varepsilon_{u_2}(1 - i0)} e^{-i\omega_{u_2}(t_{u_2} - t_{c_2})} (-i) \Xi(x_{c_1}, x_{c_2}, x_{s_1}, x_{s_2}) \times \frac{i}{2\pi} \sum_{d_1} \frac{\psi_{d_1}(\boldsymbol{r}_{s_1}) \bar{\psi}_{d_1}(\boldsymbol{r}_{d_1})}{\omega_{d_1} - \varepsilon_{d_1}(1 - i0)} e^{-i\omega_{d_1}(t_{s_1} - t_{d_1})} \frac{i}{2\pi} \sum_{d_2} \frac{\psi_{d_2}(\boldsymbol{r}_{s_2}) \bar{\psi}_{d_2}(\boldsymbol{r}_{d_2})}{\omega_{d_2} - \varepsilon_{d_2}(1 - i0)} e^{-i\omega_{d_2}(t_{s_2} - t_{d_2})} e^{-i t_{d_1}(E_{A_0} + \omega)} \delta(t_{d_1} - t_{d_2}) \Phi_{A_0}(\boldsymbol{r}_{d_1}, \boldsymbol{r}_{d_2}). \tag{79}$$

In the lowest order of perturbation theory Eqs. (73) and (74) follow from Eq. (79) if we set

$$\Xi(\boldsymbol{r}_{c_1}, \boldsymbol{r}_{c_2}, \boldsymbol{r}_{s_1}, \boldsymbol{r}_{s_2}) = 2e \gamma^{\mu_1} A^{(k_0,\lambda_0)*}_{\mu_1}(\boldsymbol{r}_{c_1}) \delta(\boldsymbol{r}_{c_1} - \boldsymbol{r}_{s_1}) \delta(\boldsymbol{r}_{c_2} - \boldsymbol{r}_{s_2}). \tag{80}$$

Consider now Eq. (79) with Ξ given by Eqs. (78) and (80), respectively. After integration over the time variables we receive

$$S = S^{\mathrm{l}} + S^{\mathrm{r}} = (-i)^3 \left(\frac{i}{2\pi}\right)^4 (2\pi)^3 \int d\omega_{u_1} d\omega_{u_2} d\omega_{d_1} d\omega_{d_2} \Delta_{82}$$
$$\times T^{+}_{A_0 u_1 u_2} 2eA^{(k_0,\lambda_0)*}_{u_1 d_1} \delta_{u_2 d_2} T_{d_1 d_2 A_0}$$
$$\times [\omega_{u_1} - \varepsilon_{u_1}(1-i0)]^{-1} [\omega_{u_2} - \varepsilon_{u_2}(1-i0)]^{-1}$$
$$\times [\omega_{d_1} - \varepsilon_{d_1}(1-i0)]^{-1} [\omega_{d_2} - \varepsilon_{d_2}(1-i0)]^{-1}, \tag{81}$$

where

$$\Delta_{82} = \delta(E_{A_0} + \omega' - \omega_{u_1} - \omega_{u_2}) \delta(\omega_{u_1} + \omega_{u_2} + \omega_0 - \omega_{d_1} - \omega_{d_2})$$
$$\times \delta(\omega_{d_1} + \omega_{d_2} - E_{A_0} - \omega) \tag{82}$$

and $\delta_{u_2 d_2}$ is the Kronecker symbol. The employment of equalities analogous to Eq. (63) yields

$$\Delta_{82} [\omega_{u_1} - \varepsilon_{u_1}(1-i0)]^{-1} [\omega_{u_2} - \varepsilon_{u_2}(1-i0)]^{-1}$$
$$\times [\omega_{d_1} - \varepsilon_{d_1}(1-i0)]^{-1} [\omega_{d_2} - \varepsilon_{d_2}(1-i0)]^{-1}$$
$$= \Delta_{82} [E_{A_0} + \omega' - \varepsilon_{u_1} - \varepsilon_{u_2}]^{-1} [E_{A_0} + \omega - \varepsilon_{d_1} - \varepsilon_{d_2}]^{-1}$$
$$\times \left(\frac{2\pi}{i}\right)^2 \delta(\omega_{u_2} - \varepsilon_{u_2}) \delta(\omega_{d_2} - \varepsilon_{d_2}) + \Delta_{82} R. \tag{83}$$

The term $\Delta_{82}R$ is again understood as in Eq. (70) above as shorthand notation for the regular part.

Insertion of Eq. (83) into Eq. (81) leads to the expression

$$S = (-2\pi i) \delta(\omega - \omega_0 - \omega') T^{+}_{A_0 u_1 u_2} [E_{A_0} + \omega' - \varepsilon_{u_1} - \varepsilon_{u_2}]^{-1}$$
$$\times \Xi_{u_1 u_2 d_1 d_2} [E_{A_0} + \omega - \varepsilon_{d_1} - \varepsilon_{d_2}]^{-1} T_{d_1 d_2 A_0}, \tag{84}$$

where

$$\Xi_{u_1 u_2 d_1 d_2} = 2eA^{(k_0,\lambda_0)*}_{u_1 d_1} \delta_{u_2 d_2}. \tag{85}$$

We also suppose that $E_I^{(0)} = \varepsilon_{d_1} + \varepsilon_{d_2}$ and $E_F^{(0)} = \varepsilon_{u_1} + \varepsilon_{u_2}$, otherwise, this term is absent. Equation (84) together with Eq. (6) gives expression for the amplitude of process [Eq. (33)]. With the use of Eq. (35) one obtains the expression for the transition amplitude. In zeroth order the eigenfunctions Φ_I, Φ_F are given by combinations of the Dirac functions in the j-j coupling scheme.

This was the goal of our derivations in this section: to express the amplitude in the form equivalent to Eq. (34). This presentation of the amplitude will help us to solve the problem of the transition probabilities for the quasidegenerate states. For the solution of this problem we need to present all the expressions in the generic matrix form [Eq. (34)].

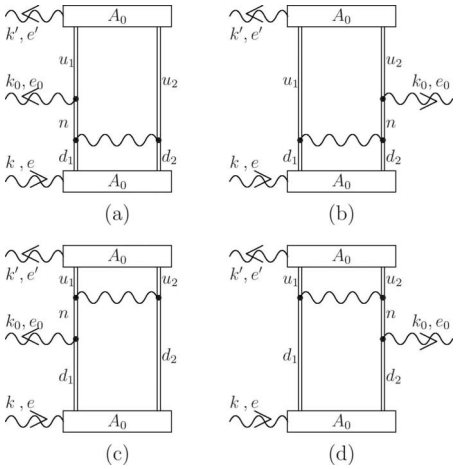

FIG. 13. The Feynman graph representing the process of elastic photon scattering on the two-electron ion. This graph includes the one-photon exchange correction and, accordingly, it represents the next order of the perturbation theory (photon exchange correction) compared to the graph (Fig. 11).

C. Two-electron ion: First-order perturbation theory (one-photon exchange)

Now, we go over to the next order corrections to the transition probabilities and consider the one-photon exchange correction. This correction is represented by the graph in Fig. 13(a). The corresponding S-matrix element can be written as

$$S = (-i)^2 \int d^4x_1 d^4x_2 d^4x_{u_1} d^4x_{u_2} d^4x_{c_1} d^4x_{d_1} d^4x_{d_2} d\omega_{u_1} d\omega_{u_2} d\omega_{d_1} d\omega_{d_2} d\omega_n d\Omega \bar{\Phi}_{A_0}(\boldsymbol{r}_{u_1}, \boldsymbol{r}_{u_2}) e^{it_{u_1}(E_{A_0}+\omega')} \delta(t_{u_1} - t_{u_2})$$
$$\times \frac{i}{2\pi} \sum_{u_1} \frac{\psi_{u_1}(\boldsymbol{r}_{u_1}) \bar{\psi}_{u_1}(\boldsymbol{r}_{c_1})}{\omega_{u_1} - \varepsilon_{u_1}(1-i0)} e^{-i\omega_{u_1}(t_{u_1} - t_1)} \frac{i}{2\pi} \sum_{u_2} \frac{\psi_{u_2}(\boldsymbol{r}_{u_2}) \bar{\psi}_{u_2}(\boldsymbol{r}_2)}{\omega_{u_2} - \varepsilon_{u_2}(1-i0)} e^{-i\omega_{u_2}(t_{u_2} - t_2)}$$
$$\times (-ie) \gamma^{\mu_{c_1}} A^{(k_0,\lambda_0)*}_{\mu_{c_1}}(\boldsymbol{r}_{c_1}) e^{i\omega_0 t_{c_1}} \frac{i}{2\pi} \sum_n \frac{\psi_n(\boldsymbol{r}_{c_1}) \bar{\psi}_n(\boldsymbol{r}_1)}{\omega_n - \varepsilon_n(1-i0)} e^{-i\omega_n(t_1 - t_2)} (-ie)^2 \frac{i}{2\pi} \gamma^{\mu_1} \gamma^{\mu_2} I_{\mu_2 \mu_3}(|\Omega|, r_{12}) e^{-i\Omega(t_1 - t_2)}$$
$$\times \frac{i}{2\pi} \sum_{d_1} \frac{\psi_{d_1}(\boldsymbol{r}_1) \bar{\psi}_{d_1}(\boldsymbol{r}_{d_1})}{\omega_{d_1} - \varepsilon_{d_1}(1-i0)} e^{-i\omega_{d_1}(t_1 - t_{d_1})} \frac{i}{2\pi} \sum_{d_2} \frac{\psi_{d_2}(\boldsymbol{r}_2) \bar{\psi}_{d_2}(\boldsymbol{r}_{d_2})}{\omega_{d_2} - \varepsilon_{d_2}(1-i0)} e^{-i\omega_{d_2}(t_2 - t_{d_2})} e^{-it_{d_1}(E_{A_0}+\omega)} \delta(t_{d_1} - t_{d_2}) \Phi_{A_0}(\boldsymbol{r}_{d_1}, \boldsymbol{r}_{d_2}), \tag{86}$$

where $r_{12} = |\boldsymbol{r}_1 - \boldsymbol{r}_2|$ and the expressions for $I_{\mu_1 \mu_2}(|\Omega|, r_{12}) \equiv I^{\mathrm{c,t}}_{\mu_1 \mu_2}(|\Omega|, r_{12})$ are defined in Coulomb gauge as

$$I^{c}_{\mu_1\mu_2}(\Omega, r_{12}) = \frac{\delta_{\mu_1 0}\delta_{\mu_2 0}}{r_{12}}, \tag{87}$$

$$I^{t}_{\mu_1\mu_2}(\Omega, r_{12}) = -\left(\frac{\delta_{\mu_1\mu_2}}{r_{12}}e^{i\Omega r_{12}} + \frac{\partial}{\partial x_1^{\mu_1}}\frac{\partial}{\partial x_2^{\mu_2}}\frac{1}{r_{12}}\frac{1-e^{i\Omega r_{12}}}{\Omega^2}\right)(1-\delta_{\mu_1 0})(1-\delta_{\mu_2 0}) \tag{88}$$

or in Feynman gauge as

$$I_{\mu_1\mu_2}(\Omega, r_{12}) = \frac{g_{\mu_1\mu_2}}{r_{12}}e^{i\Omega r_{12}}. \tag{89}$$

We will also employ the following notation for the matrix element:

$$I^{c,t}_{a'b'ab}(\Omega) = \int d^3\boldsymbol{r}_1 d^3\boldsymbol{r}_2 \bar{\psi}_{a'}(\boldsymbol{r}_1)\bar{\psi}_{b'}(\boldsymbol{r}_2)\gamma_1^{\mu_1}\gamma_2^{\mu_2} I^{c,t}_{\mu_1\mu_2}(\Omega, r_{12})\psi_a(\boldsymbol{r}_1)\psi_b(\boldsymbol{r}_2). \tag{90}$$

In Eq. (86) again the additional electron propagator (sum over n) is artificially introduced with the same purpose as in Sec. III B.

Integration over the time variables in Eq. (86) yields

$$\begin{aligned} S = (-i)^5\left(\frac{i}{2\pi}\right)^6(2\pi)^5 \int & d^3\boldsymbol{r}_1 d^3\boldsymbol{r}_2 d^3\boldsymbol{r}_{u_1} d^3\boldsymbol{r}_{u_2} d^3\boldsymbol{r}_{c_1} d^3\boldsymbol{r}_{d_1} d^3\boldsymbol{r}_{d_2} d\omega_{u_1} d\omega_{u_2} d\omega_{d_1} d\omega_{d_2} d\omega_n d\Omega \bar{\Phi}_{A_0}(\boldsymbol{r}_{u_1}, \boldsymbol{r}_{u_2})\Delta_{92} \\ \times \sum_{u_1} \frac{\psi_{u_1}(\boldsymbol{r}_{u_1})\bar{\psi}_{u_1}(\boldsymbol{r}_{c_1})}{\omega_{u_1} - \varepsilon_{u_1}(1-i0)} \sum_{u_2} \frac{\psi_{u_2}(\boldsymbol{r}_{u_2})\bar{\psi}_{u_2}(\boldsymbol{r}_2)}{\omega_{u_2} - \varepsilon_{u_2}(1-i0)} e\gamma^{\mu_{c_1}} A^{(k_0,\lambda_0)*}_{\mu_{c_1}}(\boldsymbol{r}_{c_1}) \sum_n \frac{\psi_n(\boldsymbol{r}_{c_1})\bar{\psi}_n(\boldsymbol{r}_1)}{\omega_n - \varepsilon_n(1-i0)} e^2\gamma^{\mu_1}\gamma^{\mu_2} I_{\mu_1\mu_2}(|\Omega|, r_{12}) \\ \times \sum_{d_1} \frac{\psi_{d_1}(\boldsymbol{r}_1)\bar{\psi}_{d_1}(\boldsymbol{r}_{d_1})}{\omega_{d_1} - \varepsilon_{d_1}(1-i0)} \sum_{d_2} \frac{\psi_{d_2}(\boldsymbol{r}_2)\bar{\psi}_{d_2}(\boldsymbol{r}_{d_2})}{\omega_{d_2} - \varepsilon_{d_2}(1-i0)} \Phi_{A_0}(\boldsymbol{r}_{d_1}, \boldsymbol{r}_{d_2}), \end{aligned} \tag{91}$$

where

$$\begin{aligned} \Delta_{92} = & \delta(E_{A_0} + \omega' - \omega_{u_1} - \omega_{u_2})\delta(\omega_{u_1} + \omega_0 - \omega_n) \\ & \times \delta(\omega_n - \Omega - \omega_{d_1})\delta(\omega_{u_2} + \Omega - \omega_{d_2}) \\ & \times \delta(-E_{A_0} - \omega + \omega_{d_1} + \omega_{d_2}). \end{aligned} \tag{92}$$

Accordingly, in Eq. (91) we can set

$$\omega_{u_1} = E_{A_0} + \omega' - \omega_{u_2}, \tag{93}$$

$$\omega_{d_1} = E_{A_0} + \omega - \omega_{d_2}, \tag{94}$$

$$\omega_n = E_{A_0} + \omega - \omega_{u_2}. \tag{95}$$

Investigating the position of resonances near

$$\omega' = -E_{A_0} + E_F^{(0)}, \tag{96}$$

$$\omega = -E_{A_0} + E_I^{(0)}, \tag{97}$$

one can separate out those terms in Eq. (91) that become singular near these resonances with the aid of the following sequence of equations [compare with Eq. (63)]:

$$\begin{aligned} & \Delta_{92}[\omega_{u_1} - \varepsilon_{u_1}(1-i0)]^{-1}[\omega_{u_2} - \varepsilon_{u_2}(1-i0)]^{-1}[\omega_n - \varepsilon_n(1-i0)]^{-1}[\omega_{d_1} - \varepsilon_{d_1}(1-i0)]^{-1}[\omega_{d_2} - \varepsilon_{d_2}(1-i0)]^{-1} \\ & = \Delta_{92}[E_{A_0} + \omega' - \varepsilon_{u_1} - \varepsilon_{u_2}]^{-1}\frac{2\pi}{i}\delta(\omega_{u_2} - \varepsilon_{u_2})[E_{A_0} + \omega - \varepsilon_n - \varepsilon_{u_2}]^{-1} \\ & \times \left\{\frac{2\pi}{i}\delta(\omega_{d_2} - \varepsilon_{d_2})[E_{A_0} + \omega - \varepsilon_{d_1} - \varepsilon_{d_2}]^{-1} - [E_{A_0} + \omega - \omega_{d_2} - \varepsilon_{d_1}(1-i0)]^{-1}[-\omega_{d_2} + \varepsilon_{d_2} + i0\varepsilon_{d_2}]^{-1}\right\} + \Delta_{92}R. \end{aligned} \tag{98}$$

Here R represents the terms which are regular in the vicinity of the resonances given by Eqs. (96) and (97). The first term in the curly brackets possesses a singularity [at the resonance; Eq. (97)] either in the case of $\varepsilon_{d_1}+\varepsilon_{d_2}=E_I^{(0)}$ or in the case of $\varepsilon_n+\varepsilon_{u_2}=E_I^{(0)}$. The second term becomes singular only in the latter case.

Introducing the variable

$$x=\omega_{d_2}-\varepsilon_{u_2} \tag{99}$$

we rewrite the S-matrix element S^{ld} corresponding to the Feynman graph [Fig. 13(a)] in the form

$$S^{\mathrm{ld}}=(-2\pi i)\delta(\omega'+\omega_0-\omega)T^{+}_{A_0u_1u_2}[E_{A_0}+\omega'-\varepsilon_{u_1}-\varepsilon_{u_2}]^{-1}\sum_n eA^{(k_0,\lambda_0)*}_{u_1n}$$
$$\times\Bigg\{e^2I_{nu_2d_1d_2}(|\varepsilon_{d_2}-\varepsilon_{u_2}|)[E_{A_0}+\omega-\varepsilon_n-\varepsilon_{u_2}]^{-1}[E_{A_0}+\omega-\varepsilon_{d_1}-\varepsilon_{d_2}]^{-1}-e^2\frac{i}{2\pi}\int dxI_{nu_2d_1d_2}(|x|)[x-\varepsilon_{d_2}+\varepsilon_{u_2}-i0\varepsilon_{d_2}]^{-1}$$
$$\times[x-E_{A_0}-\omega+\varepsilon_{d_1}+\varepsilon_{u_2}-i0\varepsilon_{d_1}]^{-1}[E_{A_0}+\omega-\varepsilon_n-\varepsilon_{u_2}]^{-1}\Bigg\}T_{d_1d_2A_0}. \tag{100}$$

The first term in the curly brackets has usually simple poles at two different points or it has a singularity of the second order if the points coincide. This term represents the first term of the geometric progression built for the initial state I (see [47] for details). Summation of the geometric progression results in a shift of the position of the resonance corresponding to the initial state and, accordingly, in a correction to the eigenvector of the initial state (Ψ_I) [see Eq. (35)]. As this term is taken into account while we generate the geometric progression, it does not contribute to the vertex operator and we can omit it here.

Proceeding in a similar way for the evaluation of the S-matrix element S^{rd}, corresponding to the Feynman graph [Fig. 13(b)], we get

$$S^{\mathrm{rd}}=(-2\pi i)\delta(\omega'+\omega_0-\omega)T^{+}_{A_0u_1u_2}[E_{A_0}+\omega'-\varepsilon_{u_1}-\varepsilon_{u_2}]^{-1}$$
$$\times\sum_n eA^{(k_0,\lambda_0)*}_{u_2n}\Bigg\{e^2I_{u_1nd_1d_2}(|\varepsilon_{u_1}-\varepsilon_{d_1}|)[E_{A_0}+\omega-\varepsilon_{u_1}-\varepsilon_n]^{-1}[E_{A_0}+\omega-\varepsilon_{d_1}-\varepsilon_{d_2}]^{-1}$$
$$-e^2\frac{i}{2\pi}\int dxI_{u_1nd_1d_2}(|x|)[x-\varepsilon_{d_1}+\varepsilon_{u_1}-i0\varepsilon_{d_1}]^{-1}[x-E_{A_0}-\omega+\varepsilon_{d_2}+\varepsilon_{u_1}-i0\varepsilon_{d_2}]^{-1}[E_{A_0}+\omega-\varepsilon_{u_1}-\varepsilon_n]^{-1}\Bigg\}T_{d_1d_2A_0}. \tag{101}$$

Note that the graphs in Figs. 13(a) and 13(b) give equal contributions (for $\varepsilon_{d_1}+\varepsilon_{d_2}=E_I^{(0)}$ and $\varepsilon_{u_1}+\varepsilon_n=E_I^{(0)}$, respectively). Accordingly, the equality $S^{\mathrm{ld}}=S^{\mathrm{rd}}$ holds. The vertices corresponding to the graphs [Figs. 13(a) and 13(b)] look like

$$\Xi^{(1)\mathrm{ld}}_{u_1u_2d_1d_2}=\sum_n eA^{(k_0,\lambda_0)*}_{u_1n}\delta_{\varepsilon_n+\varepsilon_{u_2},E_I^{(0)}}\Bigg[-e^2\frac{i}{2\pi}\int dxI_{nu_2d_1d_2}(|x|)$$
$$\times[x-\varepsilon_{d_2}+\varepsilon_{u_2}-i0\varepsilon_{d_2}]^{-1}$$
$$\times[x-E_{A_0}-\omega+\varepsilon_{d_1}+\varepsilon_{u_2}-i0\varepsilon_{d_1}]^{-1}\Bigg] \tag{102}$$

$$=(\Xi^{(0)}K^{(1)\mathrm{ld}})_{u_1u_2d_1d_2}, \tag{103}$$

$$\Xi^{(1)\mathrm{rd}}_{u_1u_2d_1d_2}=\sum_n eA^{(k_0,\lambda_0)*}_{u_2n}\delta_{\varepsilon_n+\varepsilon_{u_1},E_I^{(0)}}\Bigg[-e^2\frac{i}{2\pi}\int dxI_{u_1nd_1d_2}(|x|)$$
$$\times[x-\varepsilon_{d_1}+\varepsilon_{u_1}-i0\varepsilon_{d_1}]^{-1}$$
$$\times[x-E_{A_0}-\omega+\varepsilon_{d_2}+\varepsilon_{u_1}-i0\varepsilon_{d_2}]^{-1}\Bigg] \tag{104}$$

$$=(\Xi^{(0)}K^{(1)\mathrm{rd}})_{u_1u_2d_1d_2}, \tag{105}$$

where $\Xi^{(0)}$ is given by Eq. (85). Here we have introduced matrices $K^{(1)\mathrm{ld}}$ and $K^{(1)\mathrm{rd}}$ for abbreviation of the matrix elements in the square brackets. Note that if the initial state is well isolated the terms which do not match the condition $\varepsilon_{d_1}+\varepsilon_{d_1}=E_I^{(0)}$ are smaller by one order of perturbation theory and can be omitted. Accordingly, the matrices K become diagonal.

As it was done for the zeroth-order corrections, expressions (100) and (101) should be cast into the form [Eq. (34)]. For this purpose consider the graph [Fig. 14(a)]. The complicated vertex Ξ has been already composed in the zeroth order [Eq. (85)]. Our goal is now to evaluate the interelectron interaction corrections to the vertex Ξ. For that we will investigate the modification of a generic complicated vertex Ξ^{gen} after taking into account the interelectron interaction [Fig. 14(a)]. The S-matrix element corresponding to Fig. 14(a) in the first order of perturbation theory in the interelectron interaction looks like

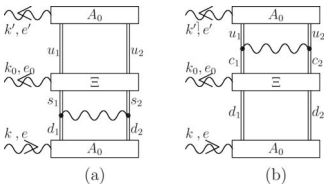

FIG. 14. The Feynman graphs representing the process of elastic photon scattering on the two-electron ion. In the lowest order of the perturbation theory these graphs reduce to the graphs (Fig. 13).

$$
\begin{aligned}
S = (-i)^2 \int & d^4x_1 d^4x_2 d^4x_{u_1} d^4x_{u_2} d^4x_{c_1} d^4x_{c_2} d^4x_{s_1} d^4x_{s_2} d^4x_{d_1} d^4x_{d_2} d\omega_{u_1} d\omega_{u_2} d\omega_{s_1} d\omega_{s_2} d\omega_{d_1} d\omega_{d_2} d\Omega \bar{\Phi}_{A_0}(\boldsymbol{r}_{u_1}, \boldsymbol{r}_{u_2}) e^{it_{u_1}(E_{A_0}+\omega')} \\
& \times \delta(t_{u_1} - t_{u_2}) \frac{i}{2\pi} \sum_{u_1} \frac{\psi_{u_1}(\boldsymbol{r}_{u_1}) \bar{\psi}_{u_1}(\boldsymbol{r}_{c_1})}{\omega_{u_1} - \varepsilon_{u_1}(1-i0)} e^{-i\omega_{u_1}(t_{u_1}-t_{c_1})} \frac{i}{2\pi} \sum_{u_2} \frac{\psi_{u_2}(\boldsymbol{r}_{u_2}) \bar{\psi}_{u_2}(\boldsymbol{r}_{c_2})}{\omega_{u_2} - \varepsilon_{u_2}(1-i0)} e^{-i\omega_{u_2}(t_{u_2}-t_{c_2})} (-i) \Xi^{\mathrm{gen}}(\boldsymbol{r}_{c_1}, \boldsymbol{r}_{c_2}, \boldsymbol{r}_{s_1}, \boldsymbol{r}_{s_2}) e^{i\omega_0 t_{c_1}} \\
& \times \delta(t_{c_1} - t_{c_2}) \delta(t_{c_1} - t_{s_1}) \delta(t_{s_1} - t_{s_2}) \frac{i}{2\pi} \sum_{s_1} \frac{\psi_{s_1}(\boldsymbol{r}_{s_1}) \bar{\psi}_{s_1}(\boldsymbol{r}_1)}{\omega_{s_1} - \varepsilon_{s_1}(1-i0)} e^{-i\omega_{s_1}(t_{s_1}-t_1)} \frac{i}{2\pi} \sum_{s_2} \frac{\psi_{s_2}(\boldsymbol{r}_{s_2}) \bar{\psi}_{s_2}(\boldsymbol{r}_2)}{\omega_{s_2} - \varepsilon_{s_2}(1-i0)} e^{-i\omega_{s_2}(t_{s_2}-t_2)} \\
& \times (-ie)^2 \frac{i}{2\pi} \gamma^{\mu_1} \gamma^{\mu_2} I_{\mu_1\mu_2}(|\Omega|, r_{1,2}) e^{-i\Omega(t_1-t_2)} \frac{i}{2\pi} \sum_{d_1} \frac{\psi_{d_1}(\boldsymbol{r}_1) \bar{\psi}_{d_1}(\boldsymbol{r}_{d_1})}{\omega_{d_1} - \varepsilon_{d_1}(1-i0)} e^{-i\omega_{d_1}(t_1-t_{d_1})} \frac{i}{2\pi} \sum_{d_2} \frac{\psi_{d_2}(\boldsymbol{r}_2) \bar{\psi}_{d_2}(\boldsymbol{r}_{d_2})}{\omega_{d_2} - \varepsilon_{d_2}(1-i0)} e^{-i\omega_{d_2}(t_2-t_{d_2})} \\
& \times e^{-it_{d_1}(E_{A_0}+\omega)} \delta(t_{d_1} - t_{d_2}) \Phi_{A_0}(\boldsymbol{r}_{d_1}, \boldsymbol{r}_{d_2}). \qquad (106)
\end{aligned}
$$

Integration over the time variables yields

$$
\begin{aligned}
S = (-i)^5 \left(\frac{i}{2\pi}\right)^7 (2\pi)^5 \int & d^3\boldsymbol{r}_1 d^3\boldsymbol{r}_2 d^3\boldsymbol{r}_{u_1} d^3\boldsymbol{r}_{u_2} d^3\boldsymbol{r}_{c_1} d^3\boldsymbol{r}_{c_2} d^3\boldsymbol{r}_{s_1} d^3\boldsymbol{r}_{s_2} d^3\boldsymbol{r}_{d_1} d^3\boldsymbol{r}_{d_2} d\omega_{u_1} d\omega_{u_2} d\omega_{s_1} d\omega_{s_2} d\omega_{d_1} d\omega_{d_2} d\Omega \bar{\Phi}_{A_0}(\boldsymbol{r}_{u_1}, \boldsymbol{r}_{u_2}) \Delta_{108} \\
& \times \sum_{u_1} \frac{\psi_{u_1}(\boldsymbol{r}_{u_1}) \bar{\psi}_{u_1}(\boldsymbol{r}_{c_1})}{\omega_{u_1} - \varepsilon_{u_1}(1-i0)} \sum_{u_2} \frac{\psi_{u_2}(\boldsymbol{r}_{u_2}) \bar{\psi}_{u_2}(\boldsymbol{r}_{c_2})}{\omega_{u_2} - \varepsilon_{u_2}(1-i0)} \Xi^{\mathrm{gen}}(\boldsymbol{r}_{c_1}, \boldsymbol{r}_{c_2}, \boldsymbol{r}_{s_1}, \boldsymbol{r}_{s_2}) \sum_{s_1} \frac{\psi_{s_1}(\boldsymbol{r}_{s_1}) \bar{\psi}_{s_1}(\boldsymbol{r}_1)}{\omega_{s_1} - \varepsilon_{s_1}(1-i0)} \sum_{s_2} \frac{\psi_{s_2}(\boldsymbol{r}_{s_2}) \bar{\psi}_{s_2}(\boldsymbol{r}_2)}{\omega_{s_2} - \varepsilon_{s_2}(1-i0)} \\
& \times e^2 \gamma^{\mu_1} \gamma^{\mu_2} I_{\mu_1\mu_2}(|\Omega|, r_{1,2}) \sum_{d_1} \frac{\psi_{d_1}(\boldsymbol{r}_1) \bar{\psi}_{d_1}(\boldsymbol{r}_{d_1})}{\omega_{d_1} - \varepsilon_{d_1}(1-i0)} \sum_{d_2} \frac{\psi_{d_2}(\boldsymbol{r}_2) \bar{\psi}_{d_2}(\boldsymbol{r}_{d_2})}{\omega_{d_2} - \varepsilon_{d_2}(1-i0)} \Phi_{A_0}(\boldsymbol{r}_{d_1}, \boldsymbol{r}_{d_2}), \qquad (107)
\end{aligned}
$$

where

$$
\Delta_{108} = \delta(E_{A_0} + \omega' - \omega_{u_1} - \omega_{u_2}) \delta(\omega_0 + \omega_{u_1} + \omega_{u_2} - \omega_{s_1} - \omega_{s_2}) \delta(-\Omega + \omega_{s_1} - \omega_{d_1}) \delta(\Omega + \omega_{s_2} - \omega_{d_2}) \delta(\omega_{d_1} + \omega_{d_2} - E_{A_0} - \omega). \qquad (108)
$$

Again we use the sequence of equations which separate out the terms (R) which are regular near the positions of the resonances under consideration [Eqs. (96) and (97)],

$$
\begin{aligned}
& \Delta_{108} [\omega_{u_1} - \varepsilon_{u_1}(1-i0)]^{-1} [\omega_{u_2} - \varepsilon_{u_2}(1-i0)]^{-1} [\omega_{s_1} - \varepsilon_{s_1}(1-i0)]^{-1} [\omega_{s_2} - \varepsilon_{s_2}(1-i0)]^{-1} [\omega_{d_1} - \varepsilon_{d_1}(1-i0)]^{-1} \\
& \quad \times [\omega_{d_2} - \varepsilon_{d_2}(1-i0)]^{-1} \\
& = \Delta_{108} \left(\frac{2\pi}{i}\right)^3 \delta(\omega_{u_2} - \varepsilon_{u_2}) \delta(\omega_{s_2} - \varepsilon_{s_2}) \delta(\omega_{d_2} - \varepsilon_{d_2}) \delta_{\varepsilon_{u_1}+\varepsilon_{u_2}, E_F^{(0)}} \delta_{\varepsilon_{s_1}+\varepsilon_{s_2}, E_I^{(0)}} \delta_{\varepsilon_{d_1}+\varepsilon_{d_2}, E_I^{(0)}} \\
& \quad \times [E_{A_0} + \omega' - \varepsilon_{u_1} - \varepsilon_{u_2}]^{-1} [E_{A_0} + \omega - \varepsilon_{s_1} - \varepsilon_{s_2}]^{-1} [E_{A_0} + \omega - \varepsilon_{d_1} - \varepsilon_{d_2}]^{-1} + \Delta_{108} \left(\frac{2\pi}{i}\right)^2 \\
& \quad \times \delta(\omega_{u_2} - \varepsilon_{u_2}) \delta(\omega_{s_2} - \varepsilon_{s_2}) \delta_{\varepsilon_{u_1}+\varepsilon_{u_2}, E_F^{(0)}} \delta_{\varepsilon_{s_1}+\varepsilon_{s_2}, E_I^{(0)}} [E_{A_0} + \omega' - \varepsilon_{u_1} - \varepsilon_{u_2}]^{-1} \\
& \quad \times [E_{A_0} + \omega - \varepsilon_{s_1} - \varepsilon_{s_2}]^{-1} [E_{A_0} + \omega - \omega_{d_2} - \varepsilon_{d_1}(1-i0)]^{-1} (-1) [-\omega_{d_2} + \varepsilon_{d_2} + i0\varepsilon_{d_2}]^{-1} + \Delta_{108} \left(\frac{2\pi}{i}\right)^2 \delta(\omega_{u_2} - \varepsilon_{u_2})
\end{aligned}
$$

$$\times\delta(\omega_{d_2}-\varepsilon_{d_2})\delta_{\varepsilon_{u_1}+\varepsilon_{u_2},E_F^{(0)}}\delta_{\varepsilon_{d_1}+\varepsilon_{d_2},E_I^{(0)}}[E_{A_0}+\omega'-\varepsilon_{u_1}-\varepsilon_{u_2}]^{-1}$$

$$\times[E_{A_0}+\omega-\omega_{s_2}-\varepsilon_{s_1}(1-i0)]^{-1}(-1)[-\omega_{s_2}+\varepsilon_{s_2}+i0\varepsilon_{s_2}]^{-1}[E_{A_0}+\omega-\varepsilon_{d_1}-\varepsilon_{d_2}]^{-1}+\Delta_{108}R. \quad (109)$$

Applying this result to Eq. (107) and combining the graphs [Figs. 12 and 14(a)] [see Eq. (84)] for the S-matrix element S^{cd}, corresponding to the Feynman graph [Fig. 14(a)] we get

$$S^{\mathrm{cd}}=(-2\pi i)\delta(\omega'+\omega_0-\omega)T^{+}_{A_0u_1u_2}[E_{A_0}+\omega'-\varepsilon_{u_1}-\varepsilon_{u_2}]^{-1}\Xi^{\mathrm{gen}}_{u_1u_2s_1s_2}\Bigg\{e^2I_{s_1s_2d_1d_2}(|\varepsilon_{s_1}-\varepsilon_{d_1}|)$$

$$\times[E_{A_0}+\omega-\varepsilon_{s_1}-\varepsilon_{s_2}]^{-1}[E_{A_0}+\omega-\varepsilon_{d_1}-\varepsilon_{d_2}]^{-1}+\Bigg[(1)_{s_1s_2d_1d_2}[E_{A_0}+\omega-\varepsilon_{d_1}-\varepsilon_{d_2}]^{-1}-e^2\frac{i}{2\pi}\int dxI_{s_1s_2d_1d_2}(|x|)$$

$$\times[x-\varepsilon_{d_1}+\varepsilon_{s_1}-i0\varepsilon_{d_1}]^{-1}[x-E_{A_0}-\omega+\varepsilon_{d_2}+\varepsilon_{s_1}-i0\varepsilon_{d_2}]^{-1}[E_{A_0}+\omega-\varepsilon_{s_1}-\varepsilon_{s_2}]^{-1}-e^2\frac{i}{2\pi}\int dxI_{s_1s_2d_1d_2}(|x|)$$

$$\times[x-\varepsilon_{d_1}+\varepsilon_{s_1}+i0\varepsilon_{s_1}]^{-1}[x-\varepsilon_{d_1}+E_{A_0}+\omega-\varepsilon_{s_2}+i0\varepsilon_{s_2}]^{-1}[E_{A_0}+\omega-\varepsilon_{d_1}-\varepsilon_{d_2}]^{-1}\Bigg]\Bigg\}T_{d_1d_2A_0}. \quad (110)$$

The first term in the curly brackets has singularities at

$$\omega'=-E_{A_0}+\varepsilon_{u_1}+\varepsilon_{u_2}, \quad (111)$$

$$\omega=-E_{A_0}+\varepsilon_{s_1}+\varepsilon_{s_2}, \quad (112)$$

$$\omega=-E_{A_0}+\varepsilon_{d_1}+\varepsilon_{d_2}. \quad (113)$$

It can be considered as the first term of the geometric progression corresponding to the initial state. This progression can be summed up (see [47]). After this the position of the resonance corresponding to the initial state will include the interelectron interaction correction (one-photon exchange).

The first term in the square brackets $[(1)_{s_1s_2d_1d_2}=\delta_{s_1d_1}\delta_{s_2d_2}]$ represents the contribution of the graph [Fig. 12]. The terms in the square brackets have singularities given by Eqs. (111) and by either Eq. (112) and (113). The last two terms represent the interelectron interaction correction to the generic vertex Ξ^{gen}. The whole term in the square brackets corresponds both to the vertex Ξ^{gen} and to the vertex $T_{d_1d_2A_0}$, which represents the process of excitation of the ground state by the photon ω with transition to the excited state (I). Accordingly, the contribution of this term to the vertex Ξ^{gen} appears with the power of 1/2.

Suppose that the initial state is isolated, i.e., the admixture of the other states has a magnitude of the next order of the perturbation theory. Then, we can set

$$\varepsilon_{s_1}+\varepsilon_{s_2}=\varepsilon_{d_1}+\varepsilon_{d_2}=E_I^{(0)} \quad (114)$$

and omit the summation over s_1, s_2 in the square brackets in Eq. (110). Accordingly, the vertex Ξ^{cd} with the interelectron interaction correction given by the graph [Fig. 14(a)] will look like

$$\Xi^{\mathrm{cd}}_{u_1u_2d_1d_2}=\Xi^{\mathrm{gen}}_{u_1u_2s_1s_2}\Bigg[(1)_{s_1s_2d_1d_2}-e^2\frac{i}{2\pi}\int dxI_{s_1s_2d_1d_2}(|x|)$$

$$\times[x-\varepsilon_{d_1}+\varepsilon_{s_1}-i0\varepsilon_{d_1}]^{-1}[x-E_{A_0}-\omega+\varepsilon_{d_2}$$

$$+\varepsilon_{s_1}-i0\varepsilon_{d_2}]^{-1}-e^2\frac{i}{2\pi}\int dxI_{s_1s_2d_1d_2}(|x|)$$

$$\times[x-\varepsilon_{d_1}+\varepsilon_{s_1}+i0\varepsilon_{s_1}]^{-1}[x-\varepsilon_{d_1}+E_{A_0}+\omega$$

$$-\varepsilon_{s_2}+i0\varepsilon_{s_2}]^{-1}\Bigg]^{1/2}$$

$$=\Xi^{\mathrm{gen}}_{u_1u_2s_1s_2}([1+K^{(1)\mathrm{cd}}]^{1/2})_{s_1s_2d_1d_2}. \quad (115)$$

The last equality defines the matrix $K^{(1)\mathrm{cd}}$. Note that the correction factor appears under the square root. The term in square brackets in Eq. (110) can be equally referred to the vertex Ξ^{gen} and to the vertex $T_{d_1d_2A_0}$. Accordingly, the part of this term connected with Ξ^{gen}, thus contributing to Ξ^{cd}, is the square root of this term.

The vertex Ξ^{cd} should be equal to the sum of the contributions of Eqs. (85), (102), and (104),

$$\Xi^{\mathrm{cd}}=\Xi^{(0)}(1+K^{(1)\mathrm{ld}}+K^{(1)\mathrm{rd}}).$$

Accordingly, we derive ($\Xi^{\mathrm{d}}=\Xi^{\mathrm{gen}}$),

$$\Xi^{\mathrm{d}}=\Xi^{(0)}(1+K^{(1)\mathrm{ld}}+K^{(1)\mathrm{rd}})(1+K^{(1)\mathrm{cd}})^{-1/2}.$$

Employing an expansion

$$(1+x)^{-1/2}=1-\frac{1}{2}x+O(x^2) \quad (116)$$

and neglecting the higher-order terms we can write

$$\Xi^{\mathrm{d}} = \Xi^{(0)}\left(1 + K^{(1)\mathrm{ld}} + K^{(1)\mathrm{rd}} - \frac{1}{2}K^{(1)\mathrm{cd}}\right) + eO(\alpha^2). \tag{117}$$

Since we are interested only in the corrections of the zeroth and first orders we can set

$$\omega = -E_{A_0} + E_I. \tag{118}$$

The first-order correction to the Ξ arises in the case of the reference state, i.e., when some of the following conditions are fulfilled:

$$\varepsilon_n + \varepsilon_{u_2} = \varepsilon_{d_1} + \varepsilon_{d_2}, \tag{119}$$

$$\varepsilon_{u_1} + \varepsilon_n = \varepsilon_{d_1} + \varepsilon_{d_2}, \tag{120}$$

$$\varepsilon_{s_1} + \varepsilon_{s_2} = \varepsilon_{d_1} + \varepsilon_{d_2}. \tag{121}$$

It is possible to describe the contributions of graphs in Figs. 13(a) and 13(b) as twice the contribution of the graph in Fig. 13(a). Accordingly, the reference states are defined by Eqs. (119) and (121), respectively.

Thus, we can write

$$\begin{aligned} K^{(1)\mathrm{ld}} + K^{(1)\mathrm{rd}} - \frac{1}{2}K^{(1)\mathrm{cd}} &= 2K^{(1)\mathrm{ld}} - \frac{1}{2}K^{(1)\mathrm{cd}} \\ &= -2e^2\frac{i}{2\pi}\int dx I_{nu_2d_1d_2}(|x|)[x - \varepsilon_{d_2} + \varepsilon_{u_2} - i0\varepsilon_{d_2}]^{-2} - \left\{-e^2\frac{i}{2\pi}\int dx I_{s_1s_2d_1d_2}(|x|)\right. \\ &\left.\times[x - \varepsilon_{d_1} + \varepsilon_{s_1} - i0\varepsilon_{d_1}]^{-2} - e^2\frac{i}{2\pi}\int dx I_{s_1s_2d_1d_2}(|x|)[x - \varepsilon_{d_1} + \varepsilon_{s_1} + i0\varepsilon_{s_1}]^{-2}\right\}. \end{aligned} \tag{122}$$

This expression can be simplified with the aid of the following identities:

$$\begin{aligned} &2I_{nu_2d_1d_2}(|x|)[x - \varepsilon_{d_2} + \varepsilon_{u_2} - i0]^{-2} - I_{s_1s_2d_1d_2}(|x|) \\ &\quad\times\{[x - \varepsilon_{d_2} + \varepsilon_{u_2} - i0]^{-2} + [x - \varepsilon_{d_2} + \varepsilon_{u_2} + i0]^{-2}\} \\ &\quad= I_{nu_2d_1d_2}(|x|)\{[x - \varepsilon_{d_2} + \varepsilon_{u_2} - i0]^{-2} \\ &\qquad- [x - \varepsilon_{d_2} + \varepsilon_{u_2} + i0]^{-2}\} \\ &\quad= \left(\frac{2\pi}{i}\right)\frac{\partial}{\partial x}I_{nu_2d_1d_2}(|x|)\,\delta(x - \varepsilon_{d_2} + \varepsilon_{u_2}). \end{aligned} \tag{123}$$

Here the formula

$$\frac{1}{(x + i0)^2} - \frac{1}{(x - i0)^2} = -\frac{2\pi}{i}\frac{\partial}{\partial x}\delta(x) \tag{124}$$

was utilized.

The same procedure should be applied to Figs. 13(c), 13(d), and 14(b), where the one-photon exchange is inserted above the emission of the photon ω_0.

Finally, we can write the following expression for the vertex Ξ:

$$\Xi = \Xi^{(0)} + \Xi^{(1)} + e\mathrm{O}(\alpha^2), \tag{125}$$

where

$$\Xi^{(0)}_{u_1u_2d_1d_2} = 2eA^{(k_0,\lambda_0)*}_{u_1d_1}\delta_{u_2d_2}, \tag{126}$$

$$\begin{aligned} \Xi^{(1)}_{u_1u_2d_1d_2} = &\sum_{\substack{n \\ \varepsilon_n+\varepsilon_{u_2}=\varepsilon_{d_1}+\varepsilon_{d_2}}} e^3A^{(k_0,\lambda_0)*}_{u_1n}\frac{\partial}{\partial x}I_{nu_2d_1d_2}(|x|)|_{x=\varepsilon_{u_2}-\varepsilon_{d_2}} \\ &+ \sum_{\substack{n \\ \varepsilon_n+\varepsilon_{d_2}=\varepsilon_{u_1}+\varepsilon_{u_2}}} e^3\frac{\partial}{\partial x}I_{u_1u_2nd_2}(|x|)|_{x=\varepsilon_{d_2}-\varepsilon_{u_2}}A^{(k_0,\lambda_0)*}_{nd_1}. \end{aligned} \tag{127}$$

Equation (127) represents the reducible part of the first-order corrections, i.e., the reference state contribution.

Having constructed a general expression for the vertex Ξ we can apply the formulas derived for the generic graphs in Figs. 12 and 14 for evaluating the contributions of the graphs in Figs. 11 and 13. Now we can express these contributions via the matrix Ξ, which enables us to extend the calculations to the quasidegenerate levels. To derive the formula for the amplitude [Eq. (35)], we will have to consider separately the case of nondegenerate levels and the case of quasidegenerate levels, respectively.

IV. EVALUATION OF TRANSITION PROBABILITIES

Evaluating the transition probabilities we should distinguish nondegenerate and quasidegenerate levels. For the nondegenerate levels standard QED perturbation theory can be applied. Configurations are called quasidegenerate if they cannot be considered as being well isolated. For these configurations the interelectron interaction must be taken into account up to higher orders. Accordingly, this requires to develop a special technique.

In Secs. IV A and IV B we derive expression for the amplitude of the scattering process for nondegenerate and quasidegenerate levels, respectively. In Sec. IV C we write down the final expressions for transition probabilities suitable for numerical calculations.

A. Nondegenerate levels

Here, we will suppose that the initial and the final states are well isolated. The set of graphs in Figs. 11 and 13 should be divided into two subsets: reducible (containing the reference states) and irreducible. For the zero-order and the reducible subset of diagrams formulas (35) and (125) can be applied, where the functions Φ_I, Φ_F are given by a combination of the two-electron determinants in j-j coupling scheme. For irreducible subsets of diagrams we can apply a procedure that will be described below.

Consider the first terms in the curly brackets in Eqs. (100) and (101),

$$S^{\mathrm{ld}} = (-2\pi i)\delta(\omega' + \omega_0 - \omega) T^{+}_{A_0 u_1 u_2} [E_{A_0} + \omega' - \varepsilon_{u_1} - \varepsilon_{u_2}]^{-1} \times \Bigg\{ (-1)e^3 \sum_n{}' A^{(k_0,\lambda_0)*}_{u_1 n} [E_{A_0} + \omega - \varepsilon_{u_2} - \varepsilon_n]^{-1} I_{n u_2 d_1 d_2} \times (|\varepsilon_{d_2} - \varepsilon_{u_2}|) \Bigg\} [E_{A_0} + \omega - \varepsilon_{d_1} - \varepsilon_{d_2}]^{-1} T_{d_1 d_2 A_0}, \quad (128)$$

$$S^{\mathrm{rd}} = (-2\pi i)\delta(\omega' + \omega_0 - \omega) T^{+}_{A_0 u_1 u_2} [E_{A_0} + \omega' - \varepsilon_{u_1} - \varepsilon_{u_2}]^{-1} \times \Bigg\{ (-1)e^3 \sum_n{}' A^{(k_0,\lambda_0)*}_{u_2 n} [E_{A_0} + \omega - \varepsilon_{u_1} - \varepsilon_n]^{-1} \times I_{u_1 n d_1 d_2} (|\varepsilon_{u_1} - \varepsilon_{d_1}|) \Bigg\} [E_{A_0} + \omega - \varepsilon_{d_1} - \varepsilon_{d_2}]^{-1} T_{d_1 d_2 A_0}. \quad (129)$$

The prime at the summation symbol indicates that in Eq. (100) terms for which $\varepsilon_{d_1} + \varepsilon_{d_2} - \varepsilon_n - \varepsilon_{u_2} = 0$ [and in Eq. (101) terms, where $\varepsilon_{d_1} + \varepsilon_{d_2} - \varepsilon_{u_1} - \varepsilon_n = 0$] holds are omitted. Since the levels I, F are well isolated the expressions in the curly brackets in Eqs. (128) and (129) can be viewed as corrections to the vertex Ξ; one can also set $\omega = -E_{A_0} + E^{(0)}_I$ in the vertex. Thus, we have to take into account the following corrections:

$$\Xi^{(1)\mathrm{d}} = (-1)e^3 \sum_{n,\ \varepsilon_{d_1} + \varepsilon_{d_2} - \varepsilon_n - \varepsilon_{u_2} \neq 0} A^{(k_0,\lambda_0)*}_{u_1 n} \times [\varepsilon_{d_1} + \varepsilon_{d_2} - \varepsilon_{u_2} - \varepsilon_n]^{-1} I_{n u_2 d_1 d_2} (|\varepsilon_{d_2} - \varepsilon_{u_2}|) + (-1)e^3 \sum_{n,\ \varepsilon_{d_1} + \varepsilon_{d_2} - \varepsilon_{u_1} - \varepsilon_n \neq 0} A^{(k_0,\lambda_0)*}_{u_2 n} \times [\varepsilon_{d_1} + \varepsilon_{d_2} - \varepsilon_{u_1} - \varepsilon_n]^{-1} I_{u_1 n d_1 d_2} (|\varepsilon_{u_1} - \varepsilon_{d_1}|) \quad (130)$$

[this is the contribution of the graphs in Figs. 13(a) and 13(b)] and

$$\Xi^{(1)\mathrm{u}} = (-1)e^3 \sum_{n,\ \varepsilon_{u_1} + \varepsilon_{u_2} - \varepsilon_n - \varepsilon_{d_2} \neq 0} I_{u_1 u_2 n d_2} (|\varepsilon_{d_2} - \varepsilon_{u_2}|) \times [\varepsilon_{u_1} + \varepsilon_{u_2} - \varepsilon_{d_2} - \varepsilon_n]^{-1} A^{(k_0,\lambda_0)*}_{d_1 n} + (-1)e^3 \sum_{n,\ \varepsilon_{u_1} + \varepsilon_{u_2} - \varepsilon_{d_1} - \varepsilon_n \neq 0} I_{u_1 u_2 d_1 n} (|\varepsilon_{u_1} - \varepsilon_{d_1}|) \times [\varepsilon_{u_1} + \varepsilon_{u_2} - \varepsilon_{d_1} - \varepsilon_n]^{-1} A^{(k_0,\lambda_0)*}_{d_2 n} \quad (131)$$

[this is the contribution of the graphs in Figs. 13(c) and 13(d)]. Accordingly, for nondegenerate levels the amplitude [Eq. (35)] is given by the matrix element of

$$\Xi = \Xi^{(0)} + \Xi^{(1)} + \Xi^{(1)\mathrm{d}} + \Xi^{(1)\mathrm{u}} \quad (132)$$

evaluated with the aid of the zeroth-order wave functions corresponding to the states I and F, i.e., by means of two-electron determinants in the j-j coupling scheme.

B. Quasidegenerate levels

In Sec. IV A we introduced the vertex Ξ via expression (34). In order to derive the amplitude as defined in Eq. (35) the wave functions Φ_I, Φ_F have to be constructed. These functions are eigenvectors of the matrix V which was investigated in [47]. Diagonalization of the matrix V is a serious task because V has infinite dimension. One possible solution of this problem is the substitution by a large but finite matrix. Another strategy is the modification of a perturbation theory. Here we will concentrate on the development of a proper perturbation theory.

The perturbation theory for the case of a nondegenerate level (as well as for the case of the fully degenerate levels) is well known [65]. Here we will apply it to the case of the quasidegenerate levels. Considering N two-electron states $\{\Psi\}$ defined in the j-j coupling scheme we assume that these states are mixing with each other, i.e., they have the same symmetry and the corresponding energy levels are close to each other. Under such condition the standard perturbation theory may not work and we have to modify it. These N states compose a set $g = \{\Psi_{i_g}, i_g = 1, \ldots, N\}$. The idea is now to build an eigenvector Φ_{n_g} corresponding to a state $\Psi_{n_g} \in g$. We also suppose that all the other states (beyond the set g) are either nonmixing with the state n_g or their energy levels are far enough from the level n_g, i.e., that the set g is large enough to incorporate all the closely lying levels. Then perturbation theory will again work. Otherwise the set g has to be enlarged. Similar but not equivalent schemes were considered earlier in the frames of RMBPT [66]. Here, we apply it in QED.

It is convenient to write the matrix V in a block form,

$$V = \begin{bmatrix} V_{11} & V_{12} \\ V_{21} & V_{22} \end{bmatrix}, \quad (133)$$

where the block V_{11} is constructed entirely on the states from the set g and the block V_{22} does not contain states from the set g. The matrix V can be decomposed as

$$V = V^{(0)} + \Delta V, \tag{134}$$

where $V^{(0)}$ is a diagonal matrix (a sum of the Dirac energies). The matrix ΔV contains the small parameter α (the expansion parameter of the QED perturbation theory) and can be treated as a perturbation. In what follows we restrict ourselves to the interelectron interaction corrections. In the lowest-order these corrections reduce to the one-photon exchange correction,

$$\Delta V = \sum_{g=c,t} I^g(|b-b'|)_{a'b'ab}. \tag{135}$$

We can write the matrix V as

$$V = \begin{bmatrix} V_{11} & V_{12} \\ V_{21} & V_{22} \end{bmatrix} = \begin{bmatrix} V_{11}^{(0)} + \Delta V_{11} & \Delta V_{12} \\ \Delta V_{21} & V_{22}^{(0)} + \Delta V_{22} \end{bmatrix}. \tag{136}$$

The block matrix V_{11} is finite and can be diagonalized numerically according to

$$V_{11}^{\text{diag}} = B^+ V_{11} B. \tag{137}$$

Since in general V is a complex-valued symmetrical matrix, i.e., $V_{ij}=V_{ji}$, matrix B is a complex orthogonal matrix,

$$B^t B = I. \tag{138}$$

Here I is a unit matrix ($I_{ij}=\delta_{ij}$) of the proper dimension. The superscript t in Eq. (138) means transposition.

Compose a matrix

$$A = \begin{bmatrix} B & 0 \\ 0 & I \end{bmatrix} \tag{139}$$

which is also an orthogonal matrix

$$A^t A = I. \tag{140}$$

Acting by the matrix A on V yields

$$\tilde{V} = A^t V A = \begin{bmatrix} V_{11}^{\text{diag}} & B^t \Delta V_{12} \\ \Delta V_{21} B & V_{22} \end{bmatrix}. \tag{141}$$

Since we have supposed that the required state n_g is weakly mixing with the states not included in the set g, the matrix $\tilde{V}$ can be diagonalized with the standard procedure [65],

$$\tilde{V}^{\text{diag}} = \tilde{C}^t \tilde{V} \tilde{C}, \tag{142}$$

where the matrix $\tilde{C}$ can be built order by order. The zeroth and the first orders of the matrix $\tilde{C}$ look like

$$\tilde{C}_{ij} = \tilde{C}_{ij}^{(0)} + \tilde{C}_{ij}^{(1)} = I_{ij} + \begin{bmatrix} 0 & \dfrac{(B^t \Delta V_{12})_{ij}}{E_j - E_i} \\ \dfrac{(\Delta V_{21} B)_{ij}}{E_j - E_i} & \dfrac{(V_{22})_{ij}}{E_j - E_i} \end{bmatrix}. \tag{143}$$

The diagonalized matrices V and $\tilde{V}$ coincide, so we can write

$$V^{\text{diag}} = \tilde{V}^{\text{diag}} = (A\tilde{C})^t V (A\tilde{C}). \tag{144}$$

Accordingly, an eigenvector Φ corresponding to a basic function Ψ can be defined as

$$\Phi = A\tilde{C}\Psi. \tag{145}$$

Now we represent the state $n_g \in g$ in terms of a perturbation expansion,

$$\Phi_{n_g} = A\tilde{C}\Psi_{n_g} = \sum_{k_g \in g} B_{k_g n_g} \Psi_{k_g}^{(0)} + \sum_{\substack{k \notin g \\ l_g \in g}} (\Delta V_{21})_{k l_g} \frac{B_{l_g n_g}}{E_{n_g}^{(0)} - E_k^{(0)}} \Psi_k^{(0)}. \tag{146}$$

An expression for ΔV_{21} is given by Eq. (135). Summation over index k means the summation over all two-electron configurations (j-j coupling scheme) including the negative part of the Dirac spectrum (not included in the set g). The employment of the j-j coupling scheme is not obligatory here.

In case when the investigated state n_g is well isolated nondegenerate level and the set g consists only of this single state, i.e., $g=\{\Psi_{n_g}\}$ the matrix B is just a one-dimensional unit matrix. It is easy to ensure that formula (146) together with Eq. (125) gives the same result as Eq. (132) (taking into account only the zeroth- and first-order corrections).

We again would like to point out the QED effects that are now taken into account in the framework of the LPA and which are missing in the relativistic many-body perturbation theory (RMBPT) [50]: the first is the inclusion of the retardation [see Eq. (135)], the second is the account of the negative part of the Dirac spectrum [summation over k in Eq. (146) and over n in Eqs. (130) and (131)], and the third is the incorporation of a nonzero contribution of $\Xi^{(1)}$ in Eq. (126) (reference state contribution).

The amplitude (U) of the scattering process for quasidegenerate levels is given by Eq. (35) where the eigenvectors are defined by Eq. (146) and the vertex operator is given by Eqs. (126) and (127).

C. Transition probability

Based on the scattering amplitude U of the process $I \to F$ with emission of the photon ω the transition probability between I and F states is given by formula

$$W = \sum_{\lambda} \int \frac{d^3\boldsymbol{k}}{(2\pi)^3} (2\pi) |U|^2 \delta(E_F + \omega - E_I)$$
$$= \frac{\omega^2}{(2\pi)^2} \sum_{\lambda} \int d\boldsymbol{\nu} |U|^2, \tag{147}$$

where $\boldsymbol{\nu}=\boldsymbol{k}/|\boldsymbol{k}|$. E_I, E_F are the energies of the initial and final states, respectively. These energies comprise of the Dirac energies and the one-photon exchange corrections. For quasidegenerate levels they are given by the corresponding eigenvalues of the matrix V [Eq. (134)]. The photon frequency $\omega=|\boldsymbol{k}|$ should be set equal to $\omega=E_I-E_F$. Equation (147) defines the full transition probability, i.e., integration over all momenta of the photon ($\boldsymbol{k}$) and summation over all polarizations of the photon (λ) are performed.

The integration over $\boldsymbol{k}$ and summation over λ are taken analytically. In Eq. (147) only the photon wave functions depend on $\boldsymbol{k}$ and λ. Accordingly, in a very general way we can consider the case when

$$U^{(0)} = A^{(k,\lambda)*}_{n_1 n_2} \tag{148}$$

$$= \int d^3\boldsymbol{r}\,\bar{\psi}_{n_1}(\boldsymbol{r})\gamma^\mu A^{(k,\lambda)*}_\mu(\boldsymbol{r})\psi_{n_2}(\boldsymbol{r}), \tag{149}$$

where $A^{(k,\lambda)}_\mu(\boldsymbol{r})$ is given by Eqs. (37) and (38). The corresponding expression for the transition probability can be written as [67]

$$W^{(0)} = \frac{\omega^2}{(2\pi)^2}\sum_{jm}\{|[A^{(E)*}_{jm}(\boldsymbol{r},\omega)]_{n_1 n_2}|^2 + |[A^{(M)*}_{jm}(\boldsymbol{r},\omega)]_{n_1 n_2}|^2\}. \tag{150}$$

Here, the notation introduced in Eq. (67) is employed. The summations run over the angular momenta of the photon (j) and projections (m). The four-vector $A^{(M,E)\mu}=(V,\boldsymbol{A})$ corresponds to magnetic (M) and electric (E) photons, respectively. In the case of the magnetic photons,

$$V^{(M)}_{jm}(\boldsymbol{r},\omega) = 0, \tag{151}$$

$$\boldsymbol{A}^{(M)}_{jm}(\boldsymbol{r},\omega) = \sqrt{\frac{2\pi}{\omega}}g_j(\omega r)\boldsymbol{Y}_{jjm}(\boldsymbol{n}). \tag{152}$$

With the appropriate choice of the gauge for the electric photons we can write

$$V^{(E)}_{jm}(\boldsymbol{r},\omega) = 0, \tag{153}$$

$$\boldsymbol{A}^{(E)}_{jm}(\boldsymbol{r},\omega) = \sqrt{\frac{2\pi}{\omega}}\left\{\sqrt{\frac{j}{2j+1}}g_{j+1}(\omega r)\boldsymbol{Y}_{jj+1m}(\boldsymbol{n}) - \sqrt{\frac{j+1}{2j+1}}g_{j-1}(\omega r)\boldsymbol{Y}_{jj-1m}(\boldsymbol{n})\right\}. \tag{154}$$

In Eqs. (152) and (154) the radial functions

$$g_l(x) = 4\pi\sqrt{\frac{\pi}{2x}}J_{l+1/2}(x) \tag{155}$$

involve Bessel functions $J_{l+1/2}(x)$ that are of the first kind [68]; $\boldsymbol{Y}_{jlm}$ ($l=j-1,j,j+1$) denotes the vector spherical harmonics [69,67] depending on angles $\boldsymbol{n}=\boldsymbol{r}/|\boldsymbol{r}|$. Formulas (153) and (154) correspond to the photon wave function given by Eqs. (37) and (38), specified within the transverse gauge [50].

For the nonrelativistic limit the more convenient gauge is represented by the transformation $\boldsymbol{A}\to\boldsymbol{A}+\boldsymbol{\nu}\chi(\boldsymbol{k},t)$, $V\to V+\chi(\boldsymbol{k},t)$ with

$$\chi(\boldsymbol{k},t) = \delta(\omega-|\boldsymbol{k}|)\sqrt{\frac{j+1}{j}}Y_{jm}(\boldsymbol{\nu})e^{-i\omega t}, \tag{156}$$

where $Y_{jm}(\boldsymbol{\nu})$ is the spherical harmonics [69]. This transformation affects only electric photons. Accordingly, in the nontransverse gauge the four-vector $A^{(E)}$ appears as

$$V^{(E)}_{jm}(\boldsymbol{r},\omega) = i\sqrt{\frac{2\pi}{\omega}}\sqrt{\frac{j+1}{j}}g_j(\omega r)Y_{jm}(\boldsymbol{n}), \tag{157}$$

$$\boldsymbol{A}^{(E)}_{jm}(\boldsymbol{r},\omega) = \sqrt{\frac{2\pi}{\omega}}\sqrt{\frac{2j+1}{j}}g_{j+1}(\omega r)\boldsymbol{Y}_{jj+1m}(\boldsymbol{n}). \tag{158}$$

In the work [50] this gauge is referred as "length" gauge.

Comparing Eqs. (147) and (150) we can express the transition probability in terms of the corresponding scattering amplitudes $U^{(E,M)}_{jm}$ as

$$W = \frac{\omega^2}{(2\pi)^2}\sum_{jm}\{|U^{(E)}_{jm}(\boldsymbol{r},\omega)|^2 + |U^{(M)}_{jm}(\boldsymbol{r},\omega)|^2\}, \tag{159}$$

where $A^{(k,\lambda)}$ are substituted by $A^{(M,E)}_{jm}$. This expression was applied for the numerical calculations of the transition probabilities.

The modified amplitudes $U^{(E,M)}_{jm}$ are derived within perturbation theory. As we take into account only the corrections up to zeroth and first orders, i.e.,

$$U^{(E,M)}_{jm} = U^{(E,M)(0)}_{jm} + U^{(E,M)(1)}_{jm} + \cdots, \tag{160}$$

then the squared absolute values of $U^{(E,M)}_{jm}$ read

$$|U^{(E,M)}_{jm}|^2 = |U^{(E,M)(0)}_{jm}|^2 + 2\,\mathrm{Re}\{U^{(E,M)(0)}_{jm}U^{(E,M)(1)}_{jm}\} + |U^{(E,M)(1)}_{jm}|^2 + \cdots. \tag{161}$$

The last term in Eq. (161) already corresponds to a correction of second order and can be, accordingly, disregarded in the calculations. However, this term may serve as an estimate for the magnitude of the higher-order corrections (i.e., for the error magnitude). The contributions of this term are given in the tables as $\Delta W^{(2+)}$.

V. NUMERICAL METHODS

In the numerical calculations an ion is considered to be enclosed into a spherical box with the radius $R=60/(\alpha Z)$ (in the relativistic units), where α is the fine-structure constant and Z is the nuclear charge. The size of the box reflects the size of the volume, where the physical processes of the interest (photon emission and interelectron interaction) mainly occur for the two-electron ions with high and intermediate Z. Hence, the electron spectrum becomes discrete. The Dirac spectrum in the external field of the nucleus is constructed in terms of B splines [70,71]. We used B splines of order 8 and a grid with 50 kn.

Expression (146) for the eigenvectors Φ_{n_g} involves the zeroth- and first-order terms of the perturbation expansion. The matrix B required for the calculation of the eigenvectors Φ_{n_g} was generated perturbatively. For a given set g, these two perturbation series are independent.

The matrix V employed in the construction of the matrix B was borrowed from our work [47], where it was evaluated

TABLE I. $M1$-transition probabilities (s^{-1}) between $(1s2s)\ ^3S_1$ and $(1s1s)\ ^1S_0$ configurations. The digits in square brackets denote the power of 10.

Z	W	Ref. [48]	Ref. [50]	Ref. [52]	Expt.
6	4.867(11)[1]	4.856[1]	4.860[1]		4.857(11)[1][a]
10	1.097(7)[4]	1.087[4]	1.092[4]		1.105(18)[4][b]
18	4.798(18)[6]	4.709[6]	4.787[6]		
26	2.078(6)[8]	2.002[8]	2.075[8]		
30	8.987(21)[8]		8.981[8]	8.993[8]	
50	1.727(2)[11]		1.726[11]	1.729[11]	
54	3.852(5)[11]		3.846[11]	3.856[11]	3.92(12)[11][c]
70	5.980(10)[12]		5.968[12]	5.983[12]	
90	9.468(23)[13]		9.439[13]	9.469[13]	
100	3.193(1)[14]		3.181[14]		

[a]Schmidt *et al.* [73].
[b]Wargelin *et al.* [74].
[c]Marrus *et al.* [4].

up to the second order with respect to the interelectron interaction corrections. The matrix ΔV_{21} involved in Eq. (146) is given by Eq. (135) and includes only the first order of the interelectron interaction corrections. It was calculated in the present work.

The spatial integration in the matrix elements of the type [Eqs. (67) and (90)] is performed in spherical coordinates. The integration over the angular variables can be performed analytically, while the integration over the radial variables is performed numerically. For the numerical integration we employed Gauss-Legendre quadratures, which yield a numerical accuracy of our calculations about 0.03%.

VI. NUMERICAL RESULTS AND DISCUSSION

In Tables I–IV we present numerical results for $M1$, $M2$, and $E1$-transition probabilities for low-lying two-electron configurations in HCI. The values are given in unit s^{-1} and the digits in square brackets refer to the power of 10.

In Tables I and II we consider transition probabilities between the $(1s2s)\ ^3S_1$ configuration and the ground $(1s1s)\ ^1S_0$ configuration and between $(1s2p_{3/2})\ ^3P_2$ configuration and $(1s1s)\ ^1S_0$ configuration with emission of magnetic $M1$ and $M2$ photons, respectively. By W we denote the transition probability evaluated in this work. The frequency of the emitted photon is set equal to $\omega=E_I-E_F$, where E_I, E_F are the energies of the initial and final states, respectively. In the case of the nondegenerate levels they comprise of the Dirac energies together with one-photon corrections. Accordingly, we do not include the radiative corrections. The contributions of the negative-energy states to the amplitude are included according to Eqs. (130) and (131) when performing summation (n) over the entire Dirac spectrum. Investigation of the contribution due to the negative-energy part of the continuum was performed in [27,52,72]. For $Z \geq 18$ the set g contains configurations in the j-j coupling scheme built on $1s$ and $2s$ electrons for $(1s2s)\ ^3S_1$ configuration and on $1s$ and $2p_{3/2}$ electrons for $(1s2p_{3/2})\ ^3P_2$ configuration. For $Z \leq 10$, due to the poor convergence of the perturbation theory, the set g contains 4000 configurations. Whenever available we compare our results with data obtained in other works. The work [48] presents the first relativistic calculation of transition probabilities for the $(1s2s)\ ^3S_1 \rightarrow (1s1s)\ ^1S_0$ transition. The paper by Johnson *et al.* [50] provides a comprehensive review, where the transition probabilities are tabulated for all Z values. However, this work is performed neglecting QED effects such as retardation and the contribution arising from the derivative in the vertex operator. The work [52] is performed within the framework of the two-time Green's-function method, which is a full QED approach too. However, in this work only the nondegenerate two-electron configurations are considered. Digits in square brackets indicate the accuracy of the measured values.

TABLE II. $M2$-transition probabilities (s^{-1}) between $(1s2p_{3/2})\ ^3P_2$ and $(1s1s)\ ^1S_0$ configurations.

Z	W	Ref. [50]	Ref. [52]
5	5.016(4)[3]	5.014[3]	
10	2.258(3)[6]	2.257[6]	
18	3.145(1)[8]	3.141[8]	
26	6.515(2)[9]	6.510[9]	
30	2.104(1)[10]	2.104[10]	2.105[10]
50	1.365(1)[12]	1.365[12]	1.366[12]
54	2.560(3)[12]	2.560[12]	
70	2.148(1)[13]	2.146[13]	2.148[13]
90	1.720(1)[14]	1.718[14]	1.721[14]
100	4.165(3)[14]	4.156[14]	

In Tables III and IV we present numerical results for $E1$-transition probabilities between $(1s2p)\ ^3P_1$, $^1P_1$ and ground $(1s1s)\ ^1S_0$ two-electron configurations. This provides the first exact QED calculation of the transition probabilities for the quasidegenerate configurations. The calculation is performed within the transverse and "nontransverse" gauges for the emitted photons: W_T and W_N, respectively. The pho-

TABLE III. $E1$-transition probabilities (s^{-1}) between $(1s2p)\ ^3P_1$ and $(1s1s)\ ^1S_0$ configurations.

Z	$W_N^{1\ \mathrm{ph}}$	$W_T^{1\ \mathrm{ph}}$	W_N^{RMBPT}	W_T^{RMBPT}	W_N	$\Delta W_N^{(2+)}$	W_T	$\Delta W_T^{(2+)}$	Ref. [49]	Ref. [50]
10	3.096[9]	2.917[9]	5.211[9]	4.963[9]	5.351(140)[9]	0.003[9]	5.095[9]	0.15[9]	5.356[9]	5.356[9]
18	1.391[12]	1.370[12]	1.793[12]	1.772[12]	1.799(6)[12]		1.777[12]	0.011[12]	1.800[12]	1.799[12]
26	3.925[13]	3.898[13]	4.482[13]	4.419[13]	4.421(61)[13]		4.396[13]	0.011[13]	4.425[13]	4.421[13]
30	1.160[14]	1.154[14]	1.258[14]	1.254[14]	1.251(7)[14]		1.246[14]	0.002[14]	1.252[14]	1.251[14]
40	6.846[14]	6.826[14]	7.047[14]	7.041[14]	7.013(34)[14]		6.997[14]	0.007[14]	7.017[14]	7.011[14]
50	2.104[15]	2.101[15]	2.132[15]	2.133[15]	2.123(9)[15]		2.120[15]	0.001[15]	2.123[15]	2.120[15]
60	4.838[15]	4.832[15]	4.874[15]	4.879[15]	4.855(19)[15]		4.850[15]	0.002[15]	4.853[15]	4.845[15]
70	9.472[15]	9.463[15]	9.523[15]	9.538[15]	9.497(26)[15]		9.489[15]	0.003[15]	9.480[15]	9.460[15]
80	1.672[16]	1.671[16]	1.680[16]	1.683[16]	1.674(6)[16]		1.673[16]		1.672[16]	1.668[16]
92	3.007[16]	3.005[16]	3.020[16]	3.027[16]	3.008(12)[16]		3.006[16]			2.994[16]

ton propagator was specified in the Coulomb gauge. In the case of quasidegenerate levels the energies E_I, E_F include also interelectron interaction corrections of the second order. We considered one- and two-photon exchange corrections to the energy levels, taken from [47], and one-photon exchange corrections to the eigenvector Φ_{n_g} in Eq. (146). The contributions of the negative-energy states to the amplitude are included in Eq. (146) in the summation over k (over the complete Dirac spectrum but the set g) and in the matrix V [see Eq. (134)] in the two-photon exchange corrections. In the columns $W_{N,T}^{1\ \mathrm{ph}}$ we give the transition probabilities calculated with only one-photon exchange correction taken into account, i.e., $W_{N,T}$ is recalculated where set $\Delta V^{(2)}=0$ in Eq. (135). The columns $W_{N,T}^{\mathrm{RMBPT}}$ display results of our recalculation of the $W_{N,T}$ values within RMBPT. In the columns $\Delta W_{N,T}^{(2+)}$ an estimate for the interelectron interaction corrections of higher orders (see the end of Sec. IV C) is given. The blank fields in the columns $\Delta W_{N,T}^{(2+)}$ express that the corresponding values are smaller than the level of accuracy of the calculation. In the last two columns we give the results of Drake [49] (the application of the unified method) and the RMBPT calculations by Johnson *et al.* [50]. While in [49] the transverse gauge was used, the calculations performed in [50] for $(1s2p)\ ^3P_1$, $^1P_1$ configurations utilized a nontransverse gauge. Digits in square brackets again denote powers of 10.

The diagonalization of the matrix V_{11} [Eq. (137)] implies that we partly take into account the photon exchange corrections to all orders. This violates the gauge invariance and, accordingly, explains the deviation between W_N and W_T. This deviation also helps us to estimate the contribution of the higher-order terms in the expansions [Eqs. (146) and (135)]. This contribution is larger for small Z values, where the convergence of the perturbation theory in the interelectron interaction is poorer.

The difference between the data in the columns $W_{N,T}$ and $W_{N,T}^{\mathrm{RMBPT}}$ determines the nonradiative QED corrections. For small Z values the considered configurations are strongly mixed. The transition probabilities for $^3P_1$ levels are very sensitive to the mixing matrix B which explains the large value of the QED corrections for the small Z values. Note that the transition probability for the $^3P_1$ level is by several orders of magnitude smaller than for the $^1P_1$ level. This means that the relative correction to the decay of the $^3P_1$ level due to the change in the matrix B is essentially larger than the correction to the decay of the level $^1P_1$. For a large numbers of Z values the mixing of the configurations is small and QED corrections appear mainly as QED corrections to $(\Delta V_{21})_{kl_g}$ in the function Φ_{n_g} [see Eq. (146)].

The perturbation expansion employed for the construction of the matrix V [Eq. (134)] and the one applied in the diagonalization of V [Eq. (146)] are different. The comparison of

TABLE IV. $E1$-transition probabilities (s^{-1}) between $(1s2p)\ ^1P_1$ and $(1s1s)\ ^1S_0$ configurations.

Z	$W_N^{1\ \mathrm{ph}}$	$W_T^{1\ \mathrm{ph}}$	W_N^{RMBPT}	W_T^{RMBPT}	W_N	$\Delta W_N^{(2+)}$	W_T	$\Delta W_T^{(2+)}$	Ref. [49]	Ref. [50]
10	8.607[12]	8.071[12]	8.538[12]	8.107[12]	8.538(14)[12]	0.007[12]	8.103[12]	0.27[12]	8.851[12]	8.851[12]
18	1.069[14]	1.052[14]	1.061[14]	1.048[14]	1.061(1)[14]		1.047[14]	0.007[14]	1.071[14]	1.070[14]
26	4.611[14]	4.578[14]	4.551[14]	4.529[14]	4.553(2)[14]		4.526[14]	0.01[14]	4.570[14]	4.566[14]
30	7.857[14]	7.815[14]	7.747[14]	7.723[14]	7.754(7)[14]		7.720[14]	0.016[14]	7.773[14]	7.763[14]
40	2.234[15]	2.227[15]	2.211[15]	2.209[15]	2.215(4)[15]		2.210[15]	0.002[15]	2.216[15]	2.212[15]
50	5.096[15]	5.085[15]	5.064[15]	5.066[15]	5.074(10)[15]		5.065[15]	0.004[15]	5.071[15]	5.057[15]
60	1.013[16]	1.012[16]	1.009[16]	1.010[16]	1.011(2)[16]		1.010[16]		1.010[16]	1.006[16]
70	1.819[16]	1.817[16]	1.813[16]	1.816[16]	1.816(3)[16]		1.814[16]		1.813[16]	1.805[16]
80	3.010[16]	3.007[16]	3.002[16]	3.009[16]	3.008(6)[16]		3.006[16]	0.001[16]	3.000[16]	2.986[16]
92	5.046[16]	5.043[16]	5.034[16]	5.049[16]	5.045(11)[16]		5.041[16]	0.001[16]		5.001[16]

the columns $W_{N,T}$ and $W^{\mathrm{l\ ph}}_{N,T}$ reveals the importance of two-photon corrections to the matrix V for the convergence of the series of the perturbation theory. If we enlarge the set g by excited configurations, the values for $W^{\mathrm{l\ ph}}_{N,T}$ would approach the ones for $W_{N,T}$. However, in order to achieve good agreement for small Z, we would have to include about 4000 significant configurations in the set g. The matrix V is well investigated for the purpose of evaluating the energies of the configurations [14,47], so the evaluation of the mixing matrix B in higher orders is a more efficient technique rather than any enlargement of the set g. The technique presented for the calculation of the transition probabilities is a rigorous QED procedure, which allows for systematic improvements of the accuracy of the calculation by taking into account corrections of higher orders.

The accuracy of the presented calculations is determined by the accuracy of the numerical methods by the contribution of the omitted orders of the perturbation theories and by the radiative corrections which are not considered here. The relative accuracy of the numerical calculation is set to 0.03%. Contribution of the omitted orders of the perturbation theories can be estimated as difference between the values calculated within the different gauges, i.e., difference between the W_N and W_T columns. However, this is a very rough estimation because one of the gauges may present better convergence than the other. Partly, the contribution of the omitted orders of the perturbation theories can be estimated by the values in columns $\Delta W^{(2+)}_{N,T}$; they show that the nontransverse gauge gives considerably better convergence. To estimate the order of magnitude of the radiative corrections we suppose that they have the same order as the other QED effects, i.e., as the difference between the values in $W_{N,T}$ and $W^{\mathrm{RMBPT}}_{N,T}$ columns, respectively. Accordingly, the values of the transition probabilities calculated within the nontransverse gauge (W_N) present the most accurate data for the transition probabilities. The estimate of inaccuracy of the data is indicated by digits in round brackets.

Concluding, we can state that at present this paper provides the most extensive and the most accurate calculations of the transition probabilities in HCI with intermediate nuclear-charge numbers Z. The inclusion of radiative corrections into the LPA (which is underway) would yield the most rigorous and powerful approach to the calculation of the transition probabilities for HCI with an utmost precision.

ACKNOWLEDGMENTS

The authors acknowledge financial support from DFG, GSI, and RFBR (Grant No. 08-02-00026-a).

APPENDIX: ADIABATIC S MATRIX

Adiabatic S matrix is a modified common S matrix where adiabatic exponent $e^{-\lambda_a|t|}$ is inserted in every vertex. The adiabatic parameter λ_a is an infinitesimal quantity ($\lambda_a \to +0$). The presence of the adiabatic exponent switches off interaction with the electromagnetic field at $t=\pm\infty$. In this appendix we show that the singularities present in the common S matrix (see Sec. II) vanish completely in the adiabatic S matrix. The singularities arise when one makes insertions into the outer electron lines of the Feynman graphs.

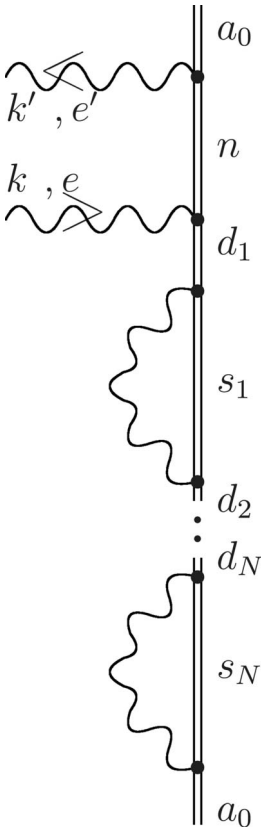

FIG. 15. The Feynman graphs representing the process of elastic photon scattering on the one-electron ion. Multiple insertions of the self-energy operator into the lower outer electron line are made in the framework of the adiabatic approximation. The break in the electron lines denotes the possible multiple insertions.

In the present paper we will consider the one-electron ions and the insertions of the self-energy operator. In the lowest order of QED perturbation-theory S-matrix element corresponding to the process of elastic photon scattering on the one-electron ions is given by the Feynman graph in Fig. 1. We consider the case when electron in the ground state a_0 absorbs photon (k,λ), then emits photon (k',λ'), and decays back to the ground state. According to energy conservation law $\omega=\omega'$. This graph gives no singularities, accordingly, the adiabatic S-matrix element coincides with the common S-matrix element,

$$S^{(0,0)} = S^{(0,0)}_{\lambda_a} = (-2\pi i)\,\delta(\omega'-\omega)e^2\sum_n \frac{A^{(k,\lambda)*}_{a_0 n} A^{(k,\lambda)}_{n a_0}}{\omega' + \varepsilon_{a_0} - \varepsilon_n}. \tag{A1}$$

The superscripts at the S matrices indicate the number of insertions of the self-energy operator into the upper and lower external electron lines. Here there are no insertions.

In the next orders of perturbation theory we have to make insertions of the self-energy operators into the electron lines. The insertions into the internal lines yield no singularities. They result in the energy shift of the excited atomic states

and were investigated in [45]. For simplicity of the derivation we omit them. Accordingly, we consider the insertions into the outer electron lines.

The N insertions of electron self-energy operators into the lower electron line are depicted in Fig. 15. After integration over time the variables with employment of equality,

$$\int_{-\infty}^{+\infty} dt e^{-\lambda_a|t|+iat} = i\left[\frac{1}{a+i\lambda_a}+\frac{1}{-a+i\lambda_a}\right], \tag{A2}$$

the corresponding adiabatic S-matrix element is given by

$$\begin{aligned}
S_{\lambda_a}^{(0,N)} = \int\, & d^3\boldsymbol{r}_u d^3\boldsymbol{r}_{d_1}\cdots d^3\boldsymbol{r}_{d_{2N}} d\omega_n d\omega_{d_1}\cdots d\omega_{d_N} d\omega_{s_1}\cdots d\omega_{s_N} d\Omega_1\cdots d\Omega_N \bar{\psi}_{a_0}(\boldsymbol{r}_u) \\
& \times(-ie)\gamma^{\mu_u} A_{\mu_u}^{(k',\lambda')*}(\boldsymbol{r}_u)\frac{i}{2\pi}\sum_n \frac{\psi_n(\boldsymbol{r}_u)\bar{\psi}_n(\boldsymbol{r}_{d_1})}{\omega_n-\varepsilon_n(1-i0)}(-ie)\gamma^{\mu_{d_1}} A_{\mu_{d_1}}^{(k,\lambda)}(\boldsymbol{r}_{d_1})(i)^2 \\
& \times\left[\frac{1}{\varepsilon_{a_0}+\omega'-\omega_n+i\lambda_a}+\frac{1}{-\varepsilon_{a_0}-\omega'+\omega_n+i\lambda_a}\right]\left[\frac{1}{\omega_n-\omega-\omega_{d_1}+i\lambda_a}+\frac{1}{-\omega_n+\omega+\omega_{d_1}+i\lambda_a}\right] \\
& \times\frac{i}{2\pi}\sum_{d_1}\frac{\psi_{d_1}(\boldsymbol{r}_{d_1})\bar{\psi}_{d_1}(\boldsymbol{r}_{d_2})}{\omega_{d_1}-\varepsilon_{d_1}(1-i0)}(-ie)\gamma^{\mu_{d_2}}\frac{i}{2\pi}\sum_{s_1}\frac{\psi_{s_1}(\boldsymbol{r}_{d_2})\bar{\psi}_{s_1}(\boldsymbol{r}_{d_3})}{\omega_{s_1}-\varepsilon_{s_1}(1-i0)} I_{\mu_{d_2}\mu_{d_3}}(|\Omega_1|,r_{d_{23}})(-ie)\gamma^{\mu_{d_3}}\psi_{a_0}(\boldsymbol{r}_{d_3})(i)^2 \\
& \times\left[\frac{1}{\omega_{d_1}-\omega_{s_1}-\Omega_1+i\lambda_a}+\frac{1}{-\omega_{d_1}+\omega_{s_1}+\Omega_1+i\lambda_a}\right]\left[\frac{1}{\omega_{s_1}+\Omega_1-\omega_{d_2}+i\lambda_a}+\frac{1}{-\omega_{s_1}-\Omega_1+\omega_{d_2}+i\lambda_a}\right]\cdots \\
& \times\frac{i}{2\pi}\sum_{d_k}\frac{\psi_{d_k}(\boldsymbol{r}_{d_{2k-1}})\bar{\psi}_{d_k}(\boldsymbol{r}_{d_{2k}})}{\omega_{d_k}-\varepsilon_{d_k}(1-i0)}(-ie)\gamma^{\mu_{d_{2k}}}\frac{i}{2\pi}\sum_{s_k}\frac{\psi_{s_k}(\boldsymbol{r}_{d_{2k}})\bar{\psi}_{s_k}(\boldsymbol{r}_{d_{2k+1}})}{\omega_{s_k}-\varepsilon_{s_k}(1-i0)} I_{\mu_{d_{2k}}\mu_{d_{2k+1}}}(|\Omega_k|,r_{d_{2k},d_{2k+1}})(-ie)\gamma^{\mu_{d_{2k+1}}}(i)^2 \\
& \times\left[\frac{1}{\omega_{d_k}-\omega_{s_k}-\Omega_k+i\lambda_a}+\frac{1}{-\omega_{d_k}+\omega_{s_k}+\Omega_k+i\lambda_a}\right]\left[\frac{1}{\omega_{s_k}+\Omega_k-\omega_{d_{k+1}}+i\lambda_a}+\frac{1}{-\omega_{s_k}-\Omega_k+\omega_{d_{k+1}}+i\lambda_a}\right]\cdots \\
& \times\frac{i}{2\pi}\sum_{d_N}\frac{\psi_{d_N}(\boldsymbol{r}_{d_{2N-1}})\bar{\psi}_{d_N}(\boldsymbol{r}_{d_{2N}})}{\omega_{d_N}-\varepsilon_{d_N}(1-i0)}(-ie)\gamma^{\mu_{d_{2N}}}\frac{i}{2\pi}\sum_{s_N}\frac{\psi_{s_N}(\boldsymbol{r}_{d_{2N}})\bar{\psi}_{s_N}(\boldsymbol{r}_{d_{2N+1}})}{\omega_{s_N}-\varepsilon_{s_N}(1-i0)} I_{\mu_{d_{2N}}\mu_{d_{2N+1}}}(|\Omega_N|,r_{d_{2N},d_{2N+1}})(-ie)\gamma^{\mu_{d_{2N+1}}}\psi_{a_0}(\boldsymbol{r}_{d_{2N+1}})(i)^2 \\
& \times\left[\frac{1}{\omega_{d_N}-\omega_{s_N}-\Omega_N+i\lambda_a}+\frac{1}{-\omega_{d_N}+\omega_{s_N}+\Omega_N+i\lambda_a}\right]\left[\frac{1}{\omega_{s_N}+\Omega_N-\varepsilon_{a_0}+i\lambda_a}+\frac{1}{-\omega_{s_N}-\Omega_N+\varepsilon_{a_0}+i\lambda_a}\right].
\end{aligned} \tag{A3}$$

In order to make the derivations shorter we will neglect the negative-energy part of the Dirac spectrum (i.e., we suppose that $\varepsilon_n>0$, $\varepsilon_d>0$) since negative-energy terms do not generate singularities.

Consider separately the integral over ω variables and designate it as F. The integrand of F includes all the terms of Eq. (A3) depending on the ω variables: the fractions in the square brackets and the denominators originating from the electron propagators. Integration over ω_n and $\omega_{s_{1,\ldots,N}}$ yields

$$\begin{aligned}
F = \int\, & d\omega_{d_1}\cdots d\omega_{d_N}\frac{2\pi}{i}\frac{1}{\omega+\omega_{d_1}-\varepsilon_n+i\lambda_a}\left[\frac{1}{\varepsilon_{a_0}+\omega'-\omega-\omega_{d_1}+2i\lambda_a}+\frac{1}{-\varepsilon_{a_0}+\omega'+\omega+\omega_{d_1}+2i\lambda_a}\right] \\
& \times\frac{2\pi}{i}\frac{1}{[\omega_{d_1}-\varepsilon_{d_1}(1-i0)](\omega_{d_2}-\varepsilon_{s_1}-\Omega_1+i\lambda_a)}\left[\frac{1}{\omega_{d_1}-\omega_{d_2}+2i\lambda_a}+\frac{1}{-\omega_{d_1}+\omega_{d_2}+2i\lambda_a}\right]\cdots \\
& \times\frac{2\pi}{i}\frac{1}{[\omega_{d_k}-\varepsilon_k(1-i0)](\omega_{d_{k+1}}-\varepsilon_{s_k}-\Omega_k+i\lambda_a)}\left[\frac{1}{\omega_{d_k}-\omega_{d_{k+1}}+2i\lambda_a}+\frac{1}{-\omega_{d_k}+\omega_{d_{k+1}}+2i\lambda_a}\right]\cdots \\
& \times\frac{2\pi}{i}\frac{1}{[\omega_{d_N}-\varepsilon_{d_N}(1-i0)](\varepsilon_{a_0}-\varepsilon_{s_N}-\Omega_N+i\lambda_a)}\left[\frac{1}{\omega_{d_N}-\varepsilon_{a_0}+2i\lambda_a}+\frac{1}{-\omega_{d_N}+\varepsilon_{a_0}+2i\lambda_a}\right].
\end{aligned} \tag{A4}$$

Integrations in Eq. (A4) can be performed recursively with the use of equality,

$$\int d\omega_{d_N} \frac{2\pi}{i} \frac{1}{[\omega_{d_{N-1}} - \varepsilon_{d_{N-1}}(1-i0)](\omega_{d_N} - \varepsilon_{s_{N-1}} - \Omega_{N-1} + i\lambda_a)} \left[\frac{1}{\omega_{d_{N-1}} - \omega_{d_N} + 2i\lambda_a} + \frac{1}{-\omega_{d_{N-1}} + \omega_{d_N} + 2i\lambda_a} \right]$$
$$\times \frac{2\pi}{i} \frac{1}{[\omega_{d_N} - \varepsilon_{d_N}(1-i0)](\varepsilon_{a_0} - \varepsilon_{s_N} - \Omega_N + i\lambda_a')} \left[\frac{1}{\omega_{d_N} - \varepsilon_{a_0} + 2i\lambda_a'} + \frac{1}{-\omega_{d_N} + \varepsilon_{a_0} + 2i\lambda_a'} \right]$$
$$= \left(\frac{2\pi}{i} \right)^3 \frac{1}{[\omega_{d_{N-1}} - \varepsilon_{d_{N-1}}(1-i0)](\varepsilon_{a_0} - \varepsilon_{d_{N-1}} - \Omega_{N-1} + 2i\lambda_a' + i\lambda_a)}$$
$$\times \left[\frac{1}{\omega_{d_{N-1}} - \varepsilon_{a_0} + 2i\lambda_a' + 2i\lambda_a} + \frac{1}{-\omega_{d_{N-1}} + \varepsilon_{a_0} + 2i\lambda_a' + 2i\lambda_a} \right] \frac{1}{(\varepsilon_{a_0} - \varepsilon_{d_N} + 2i\lambda_a')(\varepsilon_{a_0} - \varepsilon_{s_N} - \Omega_N + i\lambda_a')} + R_{\lambda_a, \lambda_a'}, \quad \text{(A5)}$$

where $\lim_{\lambda_a, \lambda_a' \to 0} R_{\lambda_a, \lambda_a'} = 0$. After integration we get the following expression for Eq. (A4):

$$F = \left(\frac{2\pi}{i} \right)^{2N+1} \left\{ \frac{1}{(\varepsilon_{a_0} - \varepsilon_{s_N} - \Omega_N + 2i\lambda_a)} \cdots \frac{1}{[\varepsilon_{a_0} - \varepsilon_{s_{N-k}} - \Omega_{N-k} + (2k+1)i\lambda_a]} \cdots \frac{1}{[\varepsilon_{a_0} - \varepsilon_{s_1} - \Omega_1 + (2N-1)i\lambda_a]} \right\}$$
$$\times \frac{1}{(\varepsilon_{a_0} - \varepsilon_{d_N} + 2i\lambda_a) \cdots (\varepsilon_{a_0} - \varepsilon_{d_{N-k+1}} + 2ki\lambda_a) \cdots (\varepsilon_{a_0} - \varepsilon_{d_1} + 2Ni\lambda_a)} \frac{1}{\omega + \varepsilon_{a_0} - \varepsilon_n + (2N+1)i\lambda_a}$$
$$\times \left[\frac{1}{\omega - \omega' + 2(N+1)i\lambda_a} + \frac{1}{-\omega + \omega' + 2(N+1)i\lambda_a} \right] + R_{\lambda_a}, \quad \text{(A6)}$$

where $\lim_{\lambda_a \to 0} R_{\lambda_a} = 0$. Function F is singular at $\lambda_a \to 0$ when $\varepsilon_{d_k} = \varepsilon_{a_0}$ and $k = 1, \ldots, N$. The term in square brackets in Eq. (A6) can be written as

$$\left[\frac{1}{\omega - \omega' + 2(N+1)i\lambda_a} + \frac{1}{-\omega + \omega' + 2(N+1)i\lambda_a} \right] = \frac{1}{2(N+1)} \left[\frac{1}{\frac{\omega - \omega'}{2(N+1)} + i\lambda_a} + \frac{1}{-\frac{\omega - \omega'}{2(N+1)} + i\lambda_a} \right] \quad \text{(A7)}$$

$$= \frac{1}{2(N+1)} \left(\frac{2\pi}{i} \right) \delta\left(\frac{\omega - \omega'}{2(N+1)} \right) = \left(\frac{2\pi}{i} \right) \delta(\omega - \omega'). \quad \text{(A8)}$$

Let us restrict ourselves to the case when $\varepsilon_{d_k} = \varepsilon_{a_0}$ for every $k = 1, \ldots, N$ (the derivations for the cases when some of $\varepsilon_{d_k} \neq \varepsilon_{a_0}$ can be performed by analogy). Accordingly, we write Eq. (A6) as

$$F = \left(\frac{2\pi}{i} \right)^{2N+1} \left\{ \frac{1}{(\varepsilon_{a_0} - \varepsilon_{s_N} - \Omega_N + i0) \cdots (\varepsilon_{a_0} - \varepsilon_{s_{N-k}} - \Omega_{N-k} + i0) \cdots (\varepsilon_{a_0} - \varepsilon_{s_1} - \Omega_1 + i0)} \right\} \left(\frac{1}{2i\lambda_a} \right)^N \frac{1}{N!}$$
$$\times \frac{1}{\omega + \varepsilon_{a_0} - \varepsilon_n + (2N+1)i\lambda_a} \left(\frac{2\pi}{i} \right) \delta(\omega - \omega') + R_{\lambda_a}. \quad \text{(A9)}$$

With employment of Eq. (A9) we can write Eq. (A3) as

$$S_{\lambda_a}^{(0,N)} = (-2\pi i)\, \delta(\omega - \omega') e^2$$
$$\times \sum_n \frac{A_{a_0 n}^{(k',\lambda')*} A_{n a_0}^{(k,\lambda)}}{(\omega + \varepsilon_{a_0} - \varepsilon_n + (2N+1)i\lambda_a)} \frac{1}{N!} \left(\frac{\hat{\Sigma}_{a_0 a_0}(\varepsilon_{a_0})}{2i\lambda_a} \right)^N$$
$$+ R_{\lambda_a}. \quad \text{(A10)}$$

Employing the asymptotic ($\lambda_a \to +0$) equality,

$$\sum_{N=0}^{\infty} \frac{1}{(x + Ni\lambda_a) N!} \left(\frac{\Delta}{i\lambda_a} \right)^N = \frac{1}{x + \Delta} \exp\left(\frac{\Delta}{i\lambda_a} \right), \quad \text{(A11)}$$

where $|x| > |\Delta|$ we can write

$$\sum_{N=0}^{\infty} S_{\lambda_a,N}^{(0,N)} = (-2\pi i)\delta(\omega-\omega')e^2 \times\left[\sum_n \frac{A_{a_0 n}^{(k',\lambda')*} A_{n a_0}^{(k,\lambda)}}{\omega+\varepsilon_{a_0}+\hat{\Sigma}_{a_0 a_0}(\varepsilon_{a_0})-\varepsilon_n}+R_{\lambda_a}\right] \times\exp\left(\frac{\hat{\Sigma}_{a_0 a_0}(\varepsilon_{a_0})}{2i\lambda_a}\right). \tag{A12}$$

Although the condition $|x|>|\Delta|$ is necessary for Eq. (A11), we employ Eq. (A11) for Eq. (A10) for any ω. This is considered as an analytical continuation of Eq. (A10) to the area close to the resonance and, accordingly, the entire complex plane (ω). This analytical continuation was discussed in [17].

If we insert the self-energy operator into the upper (N_u times) and lower (N_d times) outer electron lines, the similar derivations yield

$$S_{\lambda_a}^{(N_u,N_d)} = (-2\pi i)\delta(\omega-\omega')e^2\frac{1}{N_u!}\left[\frac{\hat{\Sigma}_{a_0 a_0}(\varepsilon_{a_0})}{2i\lambda_a}\right]^{N_u} \times\sum_n \frac{A_{a_0 n}^{(k',\lambda')*} A_{n a_0}^{(k,\lambda)}}{[\omega+\varepsilon_{a_0}-\varepsilon_n+(2N+1)i\lambda_a]}\frac{1}{N_d!} \times\left[\frac{\hat{\Sigma}_{a_0 a_0}(\varepsilon_{a_0})}{2i\lambda_a}\right]^{N_d}+R_{\lambda_a}, \tag{A13}$$

The value of N in the denominator can be set equal to N_u or N_d without changing the final result since it influences only the terms R_{λ_a} which disappear in the asymptotics ($\lambda_a \to +0$). Finally, we get

$$S_{\lambda_a} = \sum_{N_u,N_d=0}^{\infty} S_{\lambda_a}^{(N_u,N_d)} \tag{A14}$$

$$=(-2\pi i)\delta(\omega-\omega')e^2 \times\sum_n \frac{A_{a_0 n}^{(k',\lambda')*} A_{n a_0}^{(k,\lambda)}}{\omega+\varepsilon_{a_0}+\hat{\Sigma}_{a_0 a_0}(\varepsilon_{a_0})-\varepsilon_n} \tag{A15}$$

$$\times\exp\left(\frac{\hat{\Sigma}_{a_0 a_0}(\varepsilon_{a_0})}{i\lambda_a}\right). \tag{A16}$$

As the regularized self-energy matrix element for the ground state (a_0) has no imaginary part, the absolute value of the exponent in Eq. (A16) reads

$$\left|\exp\left(\frac{\hat{\Sigma}_{a_0 a_0}(\varepsilon_{a_0})}{i\lambda_a}\right)\right| = 1. \tag{A17}$$

Accordingly, the absolute value of the amplitude is given by

$$|U| = e^2\left|\sum_n \frac{A_{a_0 n}^{(k',\lambda')*} A_{n a_0}^{(k,\lambda)}}{\omega+\epsilon_{a_0}-\varepsilon_n}\right|. \tag{A18}$$

The regularized self-energy matrix element in the denominator is a correction to the energy of the ground state: $\epsilon_{a_0}=\varepsilon_{a_0}+\hat{\Sigma}_{a_0 a_0}(\varepsilon_{a_0})$.

In Eq. (A9) we considered only the case when $\varepsilon_{d_k}=\varepsilon_{a_0}$ for every $k=1,\ldots,N$. The cases when some of $\varepsilon_{d_k}\neq\varepsilon_{a_0}$ correspond to the insertions of the second and higher orders self-energy corrections of the "loop-after-loop" type. The case when all $\varepsilon_{d_k}\neq\varepsilon_{a_0}$ gives the correction to the wave function of the ground-state electron a_0.

The presented derivations show that the employment of the adiabatic theory allows for the insertions into the outer electron lines within the LPA. They also justify the introduction of the vertex functions Φ_{a_0}, $\bar{\Phi}_{a_0}$ (Φ_{A_0}, $\bar{\Phi}_{A_0}$ for two-electron ions) in Sec. III. The energies of the ground state can be considered to be the full energies, i.e., with all the corrections included.

Finally, we would like to note that the goal of employment of the adiabatic approach was the justification of the LPA backgrounds. Formally, the ground state can be investigated within the same matrix formulation of the LPA as the excited states which allows us to employ the general technique developed in Sec. IV.

[1] T. Stöhlker *et al.*, J. Phys.: Conf. Ser. **72**, 012008 (2007).
[2] A. Gumberidze *et al.*, Phys. Rev. Lett. **92**, 203004 (2004).
[3] J. Schweppe *et al.*, Phys. Rev. Lett. **66**, 1434 (1991).
[4] R. Marrus, A. Simionovici, P. Indelicato, D. D. Dietrich, P. Charles, J.-P. Briand, K. Finlayson, F. Bosch, D. Liesen, and F. Parente, Phys. Rev. Lett. **63**, 502 (1989).
[5] M. Zolotorev and D. Budker, Phys. Rev. Lett. **78**, 4717 (1997).
[6] V. G. Gorshkov and L. N. Labzovskii, Zh. Eksp. Teor. Fiz. Pis'ma Red. **19**, 768 (1974) [JETP Lett. **19**, 394 (1974)].
[7] A. Schäfer, G. Soff, P. Indelicato, B. Müller, and W. Greiner, Phys. Rev. A **40**, 7362 (1989).
[8] R. W. Dunford, Phys. Rev. A **54**, 3820 (1996).
[9] L. N. Labzowsky, A. V. Nefiodov, G. Plunien, G. Soff, R. Marrus, and D. Liesen, Phys. Rev. A **63**, 054105 (2001).
[10] A. V. Nefiodov, L. N. Labzowsky, D. Liesen, G. Plunien, and G. Soff, Phys. Lett. B **534**, 52 (2002).
[11] G. F. Gribakin, F. J. Currell, M. G. Kozlov, and A. I. Mikhailov, Phys. Rev. A **72**, 032109 (2005).
[12] M. Maul, A. Schäfer, and P. Indelicato, e-print arXiv:physics/9705010.
[13] M. Maul, A. Schäfer, W. Greiner, and P. Indelicato, Phys. Rev. A **53**, 3915 (1996).
[14] A. N. Artemyev, V. M. Shabaev, V. A. Yerokhin, G. Plunien,

and G. Soff, Phys. Rev. A **71**, 062104 (2005).
[15] O. Y. Andreev, L. N. Labzowsky, G. Plunien, and G. Soff, Phys. Rev. Lett. **94**, 243002 (2005).
[16] S. Schiller, Phys. Rev. Lett. **98**, 180801 (2007).
[17] O. Y. Andreev, L. N. Labzowsky, G. Plunien, and D. A. Solovyev, Phys. Rep. **455**, 135 (2008).
[18] J.-P. Desclaux, in *Relativistic Electronic Structure Theory (Part 1: Fundamentals)*, edited by P. Schwerdtfeger (Elsevier, New York, 2002), pp. 1–20.
[19] I. P. Grant and H. M. Quiney, in *Relativistic Electronic Structure Theory (Part 1: Fundamentals)*, edited by P. Schwerdtfeger (Elsevier, New York, 2002), pp. 107–194.
[20] U. Kaldor, E. Eliav, and A. Landau, in *Theoretical Chemistry and Physics of Heavy and Superheavy Elements*, edited by U. Kaldor and S. Wilson (Kluwer, Dordrecht, 2003), pp. 171–203.
[21] G. E. Brown and D. G. Ravenhall, Proc. R. Soc. London, Ser. A **208**, 552 (1951).
[22] I. P. Grant and H. M. Quiney, Adv. At. Mol. Phys. **23**, 37 (1988).
[23] M. H. Mittleman, Phys. Rev. A **5**, 2395 (1972).
[24] L. Labzowsky, G. Klimchitskaya, and Yu. Dmitriev, *Relativistic Effects in the Spectra of Atomic Systems* (Institute of Physics, Bristol, 1993).
[25] W. R. Johnson and J. Sapirstein, Phys. Rev. A **46**, R2197 (1992).
[26] D. R. Plante, W. R. Johnson, and J. Sapirstein, Phys. Rev. A **49**, 3519 (1994).
[27] A. Derevianko, I. M. Savukov, W. R. Johnson, and D. R. Plante, Phys. Rev. A **58**, 4453 (1998).
[28] M. H. Chen, K. T. Cheng, and W. R. Johnson, Phys. Rev. A **64**, 042507 (2001).
[29] I. M. Savukov, L. N. Labzowsky, and W. R. Johnson, Phys. Rev. A **72**, 012504 (2005).
[30] M. I. Eides, H. Grotch, and V. A. Shelyuto, Phys. Rep. **342**, 63 (2001).
[31] M. Gell-Mann and F. Low, Phys. Rev. **84**, 350 (1951).
[32] J. Sucher, Phys. Rev. **107**, 1448 (1957).
[33] L. N. Labzovskii, Zh. Eksp. Teor. Fiz. **59**, 168 (1970) [JETP **32**, 94 (1970)].
[34] V. M. Shabaev, Izv. Vyssh. Uchebn. Zaved. Fiz. **33**, 43 (1990) [Sov. Phys. J. **33**, 660 (1990)].
[35] V. M. Shabaev, J. Phys. A **24**, 5665 (1991).
[36] V. M. Shabaev, Phys. Rep. **356**, 119 (2002).
[37] V. A. Yerokhin and V. M. Shabaev, Phys. Rev. A **64**, 062507 (2001).
[38] V. M. Shabaev, M. Tomaselli, T. Kühl, A. N. Artemyev, and V. A. Yerokhin, Phys. Rev. A **56**, 252 (1997).
[39] V. A. Yerokhin, P. Indelicato, and V. M. Shabaev, Phys. Rev. Lett. **89**, 143001 (2002).
[40] I. Lindgren, B. Åsén, S. Salomonson, and A.-M. Mårtensson-Pendrill, Phys. Rev. A **64**, 062505 (2001).
[41] I. Lindgren, S. Salomonson, and B. Åsén, Phys. Rep. **389**, 161 (2004).
[42] F. Low, Phys. Rev. **88**, 53 (1952).
[43] L. Labzowsky, V. Karasiev, I. Lindgren, H. Persson, and S. Salomonson, Phys. Scr., T **T46**, 150 (1993).
[44] L. N. Labzowsky and M. A. Tokman, Adv. Quantum Chem. **30**, 393 (1998).
[45] O. Y. Andreev, L. N. Labzowsky, G. Plunien, and G. Soff, Phys. Rev. A **64**, 042513 (2001).
[46] O. Yu. Andreev, L. N. Labzowsky, G. Plunien, and G. Soff, Phys. Rev. A **67**, 012503 (2003).
[47] O. Y. Andreev, L. N. Labzowsky, G. Plunien, and G. Soff, Phys. Rev. A **69**, 062505 (2004).
[48] G. W. F. Drake, Phys. Rev. A **3**, 908 (1971).
[49] G. W. F. Drake, Phys. Rev. A **19**, 1387 (1979).
[50] W. R. Johnson, D. R. Plante, and J. Sapirstein, Adv. At., Mol., Opt. Phys. **35**, 255 (1995).
[51] J. Sapirstein, K. Pachucki, and K. T. Cheng, Phys. Rev. A **69**, 022113 (2004).
[52] P. Indelicato, V. M. Shabaev, and A. V. Volotka, Phys. Rev. A **69**, 062506 (2004).
[53] R. Barbieri and J. Sucher, Nucl. Phys. B **134**, 155 (1978).
[54] L. N. Labzowsky, A. Prosorov, A. V. Shonin, I. Bednyakov, G. Plunien, and G. Soff, Ann. Phys. (N.Y.) **302**, 22 (2002).
[55] L. N. Labzovskii, Zh. Eksp. Teor. Fiz. **85**, 869 (1983) [Sov. Phys. JETP **58**, 503 (1983)].
[56] L. Labzowsky, V. Karasiev, and I. Goidenko, J. Phys. B **27**, L439 (1994).
[57] L. N. Labzowsky, I. A. Goidenko, and D. Liesen, Phys. Scr. **56**, 271 (1997).
[58] L. N. Labzowsky, D. A. Solovyev, G. Plunien, and G. Soff, Phys. Rev. Lett. **87**, 143003 (2001b).
[59] U. D. Jentschura and P. J. Mohr, Can. J. Phys. **80**, 633 (2002).
[60] L. N. Labzowsky, D. A. Solovyev, G. Plunien, and G. Soff, Can. J. Phys. **80**, 1187 (2002).
[61] L. Labzowsky, D. Soloviev, G. Plunien, and G. Soff, Phys. Rev. A **65**, 054502 (2002).
[62] L. Labzowsky and D. Solovjev, Phys. Rev. A **66**, 024503 (2002).
[63] L. N. Labzowsky and D. A. Solovyev, in *Precision Physics of Simple Atomic Systems*, edited by S. G. Karshenboim and V. B. Smirnov (Springer, New York, 2003), p. 15.
[64] L. Labzowsky and D. Solovyev, J. Phys. B **37**, 3271 (2004).
[65] L. D. Landau and E. M. Lifshits, *Quantum Mechanics* (Pergamon, Oxford, 1977).
[66] V. A. Dzuba, V. V. Flambaum, and M. G. Kozlov, Phys. Rev. A **54**, 3948 (1996).
[67] A. I. Akhiezer and V. B. Berestetskii, *Quantum Electrodynamics* (Wiley, New York, 1965).
[68] M. Abramowitz and I. A. Stegun, *Handbook of Mathematical Functions With Formulas, Graphs and Mathematical Tables* (Dover, New York, 1972).
[69] D. A. Varshalovich, A. N. Moskalev, and V. K. Khersonskii, *Quantum Theory of Angular Momentum* (World Scientific, Singapore, 1988).
[70] W. R. Johnson, S. A. Blundell, and J. Sapirstein, Phys. Rev. A **37**, 307 (1988).
[71] V. M. Shabaev, I. I. Tupitsyn, V. A. Yerokhin, G. Plunien, and G. Soff, Phys. Rev. Lett. **93**, 130405 (2004).
[72] P. Indelicato, Phys. Rev. Lett. **77**, 3323 (1996).
[73] H. T. Schmidt *et al.*, Phys. Rev. Lett. **72**, 1616 (1994).
[74] B. J. Wargelin, P. Beiersdorfer, and S. M. Kahn, Phys. Rev. Lett. **71**, 2196 (1993).